

Fishers Harvest Parallel Unlearning in Inherited Model Networks

Xiao Liu*
Beijing University of Posts and
Telecommunications
Beijing, China
liuxiao68@bupt.edu.cn

Mingyuan Li*
Beijing University of Posts and
Telecommunications
Beijing, China
henryli_i@bupt.edu.cn

Xu Wang
University of Technology Sydney
Sydney, Australia
xu.wang@uts.edu.au

Guangsheng Yu†
CSIRO Data61
Sydney, Australia
saber.yu@data61.csiro.au

Wei Ni
CSIRO Data61
Sydney, Australia
wei.ni@data61.csiro.au

Lixiang Li†
Beijing University of Posts and
Telecommunications
Beijing, China
lixiang@bupt.edu.cn

Haipeng Peng
Beijing University of Posts and
Telecommunications
Beijing, China
penghaipeng@bupt.edu.cn

Ren Ping Liu
University of Technology Sydney
Sydney, Australia
renping.liu@uts.edu.au

ABSTRACT

Unlearning in various learning frameworks remains challenging, with the continuous growth and updates of models exhibiting complex inheritance relationships. This paper presents a novel unlearning framework, which enables fully parallel unlearning among models exhibiting inheritance. A key enabler is the new Unified Model Inheritance Graph (UMIG), which captures the inheritance using a Directed Acyclic Graph (DAG). Central to our framework is the new Fisher Inheritance Unlearning (FIUn) algorithm, which utilizes the Fisher Information Matrix (FIM) from initial unlearning models to pinpoint impacted parameters in inherited models. By employing FIM, the FIUn method breaks the sequential dependencies among the models, facilitating simultaneous unlearning and reducing computational overhead. We further design to merge disparate FIMs into a single matrix, synchronizing updates across inherited models. Experiments confirm the effectiveness of our unlearning framework. For single-class tasks, it achieves complete unlearning with 0% accuracy for unlearned labels while maintaining 94.53% accuracy for retained labels on average. For multi-class tasks, the accuracy is 1.07% for unlearned labels and 84.77% for retained labels on average. Our framework accelerates unlearning by 99% compared to alternative methods.

1 INTRODUCTION

The explosive growth of data volume and the increasing complexity of applications necessitate models that can constantly update to adapt to new data, constraints, and standards [21]. Accordingly, the need for data privacy, the auditing of illegal information from models, and compliance with regulations and industry standards arises. This leads to the concept of “model forgetting” or “unlearning,” which involves removing specific information from trained models.

The importance of unlearning lies in its ability to remove data that may raise privacy concerns, ensuring that the model can no longer recognize or rely on such data, in compliance with regulations such as the General Data Protection Regulation (GDPR) [56]. Additionally, unlearning plays a crucial role in data correction, removing the impact of erroneous or biased data from the model and enhancing its accuracy and fairness. This not only protects user privacy but also boosts the model’s quality and reliability, aligning with both ethical standards and legal requirements.

Machine unlearning becomes particularly challenging when models are consistently recorded with a directed acyclic graph (DAG) topology, where models inheriting from predecessors also require updates. Examples of such scenarios include a basic model being customized to meet various Machine Learning Operations (MLOps) lifecycle requirements [26, 39] or distilled to fit computational resource constraints [45].

The concept of model inheritance can be applied to prevalent learning frameworks, such as Federated Learning (FL) [30], Distributed Data-Parallel Learning (DDPL) [33], Incremental Learning (IL) [55], and Transfer Learning (TL) [58]. In this case, unlearning even a single model would need to unlearn the entire subgraph rooted at the origin to ensure all descendant models are consistent and relevant.

Research Gap. Various machine unlearning techniques have been proposed. Unfortunately, the inheritance relationships among related models prevent most existing unlearning methods from being executed in parallel, including re-training [23, 36], gradient ascent [65], or knowledge distillation methods [49]. On the other hand, Sharding, Isolation, Slicing, and Aggregated Training (SISA) [3] is a commonly used efficient method that reduces the dependence between data by dividing it into multiple segments and training multiple models in parallel. However, SISA is also inapplicable when there are inheritance relationships between models [37]. This is due to the fact that SISA needs to be performed sequentially from the starting point of updating to the end of the subgraph, incurring

*Contributed equally to this research

†Corresponding author.

significant overhead and resource consumption during unlearning. In this sense, there is a pressing need for an effective and efficient way to perform unlearning in the presence of model inheritance relationships.

Research Question. To address this research gap, we need to identify the commonalities across various prevalent frameworks in unlearning and determine how a new unlearning design can be universally applied. Specifically, we raise two key Research Questions (RQs):

RQ1. *How can unlearning requests be swiftly allocated to models that need updates and then prepare these models for unlearning tasks within a large-scale, interdependent model network?*

RQ2. *How can the model unlearning tasks be efficiently and effectively executed, especially when the unlearning of one model impacts subsequent models?*

In response to these two RQs, we investigate the topological structure and unlearning impact of inherited models in four prevalent frameworks: FL, DDPL, IL, and TL. Specifically, we study the key factors affecting the efficiency, accuracy, and consistency of model unlearning. These include the selection of model parameters, changes in data distribution, and utilization of computational resources.

Contributions. This paper presents a novel parallel unlearning framework that can conduct efficient unlearning among large numbers of dependent models with complex inheritance relations, e.g., in FL, DDPL, IL, and TL. We first propose a new Unified Model Inheritance Graph (UMIG), to unveil the inheritance characteristic among models in various learning frameworks. With the assistance of the UMIG and Fisher Information Matrix (FIM), we develop the Fisher Inheritance Unlearning (FIUn) method that can efficiently pinpoint critical model parameters to be unlearned.

This allows independent unlearning adjustments on large-scale inherited models. To further enable effective one-shot unlearning of knowledge inherited from multiple upstream, we design a merging FIM function that consolidates disparate FIMs and identifies the critical parameters that need updating across all sources.

The contributions of this paper are summarized as follows:

- We propose the UMIG, which abstracts various prevalent learning frameworks, e.g., FL, DDPL, IL, and TL, in a unified fashion using DAGs to represent models' interdependence. This facilitates the analysis of large-scale inheritance-oriented model networks.
- We design the FIUn method, which enables efficient parallel unlearning within the UMIG. The method leverages the FIM to quantify the significance of model parameters to unlearning tasks, and selectively scales the parameters according to their importance.
- We further develop the merging FIM function to consolidate the FIMs from multiple upstream unlearning models into a cohesive matrix, thereby aggregating the unlearning tasks inherited from those models. This design facilitates the one-shot removal of inherited knowledge and reduces computational overhead within the UMIG.

Comprehensive experiments demonstrate that our method achieves complete unlearning for single-class unlearning tasks across all considered learning frameworks and model types, retaining an average accuracy of 94.53%. For multi-class unlearning tasks, the average unlearning accuracy drops to 1.07%, while the accuracy for retained labels reaches up to 84.77%. Additionally, our algorithm shows a 99% speed improvement across all considered frameworks compared to alternative methods.

Paper Organization. The rest of the paper is organized as follows. Section 2 reviews the preliminaries. Section 3 provides the proposed UMIG, followed by introducing the novel FIUn method and merging FIM function in Section 4. Section 5 presents the experimental settings. Section 6 presents our comprehensive experimental results based on four learning frameworks. Section 7 reviews the related works. Section 8 concludes this work.

2 PRELIMINARIES

This section introduces the concepts, notation, and formulas of this paper, including machine unlearning and FIM.

2.1 Machine Unlearning

Machine unlearning refers to removing the influence of specific data subsets from a trained model while maintaining its performance on the remaining data [12, 54]. In other words, the goal is to eliminate the impact of specific labels on the model's predictions while ensuring that the prediction accuracy for the remaining labels and the overall performance of the model remain unaffected.

Let $D = \{(x_i, y_i)\}_{i=1}^N$ represent a dataset where x_i is the i -th training sample and $y_i \in \{1, \dots, K\}$ is the corresponding class label. Let C_f denote the set of labels to be unlearned, corresponding to the data set $D^f \subset D$ to be unlearned, and C_r represent the set of retained labels, corresponding to the remaining data set $D^r = D \setminus D^f$.

Unlearning aims to eliminate the impact of D^f with labels in C_f from the model while preserving its performance on D^r with labels in C_r . In this context, we define $\phi_\theta(\cdot) : X \rightarrow Y$ as a function parameterized by $\theta \in \mathbb{R}^m$, where $X \in \mathbb{R}^n$ and $Y \in \mathbb{R}^K$. The k -th component of $\phi_\theta(x)$ represents the probability that sample x belongs to class k . The objective is to adjust θ such that the model effectively "forgets" the influence of C_f while retaining accurate predictions on C_r .

2.2 Fisher Information Matrix

The FIM is a useful tool in statistics for assessing the accuracy of parameter estimates [16, 24]. It quantifies the impact of parameter changes on the probability distribution of observed data.

Given a probability density function $p(x|\theta)$ conditioned on the model parameter θ , an FIM $I(\theta)$ is the expected value of the second derivative of the negative log-likelihood function $\ell(\theta)$, as given by

$$I(\theta) = \mathbb{E} \left[-\frac{\partial^2 \ell(\theta)}{\partial \theta^2} \right], \text{ where } \ell(\theta) = \ln p(x|\theta). \quad (1)$$

To simplify computation, in practice, the diagonal of the FIM can approximate the second derivative of the loss function [2, 50].

An equivalent form of $I(\theta)$ is given by

$$I(\theta) = \mathbb{E} \left[\left(\left(\frac{\partial \ell(\theta)}{\partial \theta} \right) \left(\frac{\partial \ell(\theta)}{\partial \theta} \right)^\top \right) \right]. \quad (2)$$

In this paper, the FIM is employed to quantify the importance of data to the model parameters. By comparing the FIMs of the training dataset and the to-be-unlearned dataset, we can identify the critical parameters related to the knowledge that needs to be unlearned.

3 CAPTURING MODEL-INHERITANCE: UMIG

In this section, we explore the topological structure of four prevalent frameworks, FL, DDPL, IL, and TL, and analyze the impact of unlearning on the inherited models within these frameworks. We propose the UMIG, which can describe the model inheritance and update relationships in these learning frameworks in a unified manner.

3.1 Diverse Learning Frameworks and Tasks

3.1.1 Federated Learning. A central server creates a global model, which participants download to locally update the model parameters based on their local data. The participants then send back their updated parameters. The central server aggregates the parameters to update and redistribute the global model. This process repeats until the model converges [25, 34, 40]. As shown in Figure 1(a), the topology of FL consists of nodes representing model states and edges representing parameter transmission and aggregation. Updates to model A trigger updates in the global model D and then to E , F , G , and H . FL also has other structures.

Multi-layer FL. This variant introduces an intermediate aggregation layer to traditional FL [7, 32], as depicted in Figure 1(b). This approach adds multiple servers that perform intermediate aggregation between the clients and the global server, thus reducing the burden on the global server, improving system scalability, and enhancing model training.

DAG-FL. As shown in Figure 1(d), multiple clients update and aggregate models hierarchically in DAG-FL [4, 5, 62]. Each node can receive model updates from multiple parent nodes and send the updated results to multiple child nodes. This structure enables efficient model training and more flexible communication, better adapting to complex network environments and different application needs.

3.1.2 Distributed Data-Parallel Learning. Training tasks are typically segmented into multiple sub-tasks, distributed among various computing nodes or servers for execution, as documented in [1, 10, 14, 31, 44]. Each node independently processes its designated sub-task and periodically synchronizes its model parameters with others to collectively refine the global model. This iterative process is crucial, particularly in DDPL topologies – similar to the FL topology depicted in Figure 1(a) – which require the sub-tasks E , F , and H , as well as the aggregated model I , to be updated continually with each new iteration of the global model D .

3.1.3 Incremental Learning. Incremental (or “Continual”) learning entails training a model initially on a dataset and then progressively updating it as new data arrives, ensuring adaptability to the latest information [18, 46]. IL can be visualized as shown in Figure 1(c),

where nodes represent different updated states of the model, and edges depict the transition between model states after data updates. If the initial state model G continues to update, then the subsequent models A and B that receive new data, as well as their related models, also need updates.

3.1.4 Transfer Learning. TL involves pre-training a base model on one dataset and then applying this model to a new task. Typically, this process includes fine-tuning the parameters of the last few layers to better suit the new task [46, 47]. The model continues to train on the specific dataset of the new task to adapt fully to its requirements. Through ongoing fine-tuning and training, the model is optimized for the best performance on the new task. The TL topology, similar to the IL topology shown in Figure 1(c), also follows a comparable model updating process.

In these diverse learning frameworks, the inheritance relationship between models is pivotal. When a base model is updated or optimized, all corresponding child models derived from it must also be updated. To accurately capture this inheritance relationship, we employ the DAG topology as an effective abstraction method to capture the dependencies among models in these learning frameworks. The use of the DAG ensures that when a single model is updated, the entire subgraph—originating from this model and encompassing all related child models—is appropriately updated.

3.2 Unified Model Inheritance Graph (UMIG)

To uniformly handle and analyze the inheritance and update relationships of models across various learning frameworks, including FL, DDPL, IL, and TL, we propose a DAG-based UMIG. It provides a comprehensive framework to represent components such as models, data, and tasks and their interdependencies within these frameworks. It also facilitates a structured and intuitive understanding of these complex model networks. Figure 2 illustrates the ability of UMIG to depict the inheritance relationships between models.

As illustrated in Figure 2, we define a weighted directional graph $\mathcal{G} = (N, E)$. Herein, $N = \{n_1, n_2, \dots, n_m\}$ represents the model nodes in the network, more specifically, a set of model parameters in a specific state or task. Moreover, $E = \{e_{01}, e_{02}, \dots, e_{mm}\}$ represents the inheritance relationships between model nodes, encompassing parameter transfer and task inheritance. For instance, in FL and DDPL, the edges may represent the transfer of parameters from local to global models. By contrast, in TL, the edges signify the inheritance of tasks from a pre-trained model to a fine-tuned model.

Based on the source and state of the model, we further categorize the nodes into two types:

- **Discovery Nodes** refer to models trained on data with an unlearned label set, enabling these nodes to adapt to the updated classification ability within the corresponding subgraph of the DAG. The root model nodes n_s and n_f in Figure 2 belong to this type.
- **Inherited Nodes** comprise the remaining nodes in the subgraph, except the discovery nodes. Inherited nodes point to the discovery or other inherited nodes, and focus on refining classification performance. The model nodes $n_h, n_j, n_l, n_p, n_g, n_i, n_n$ belong to this type.

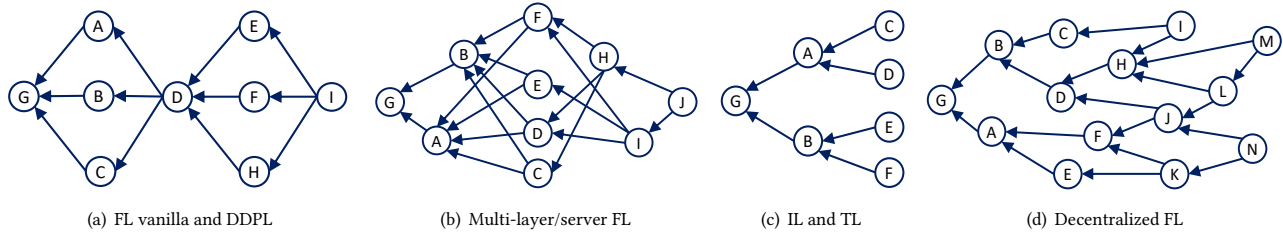


Figure 1: These diagrams demonstrate various learning frameworks that can be constituted to the proposed UMIG.

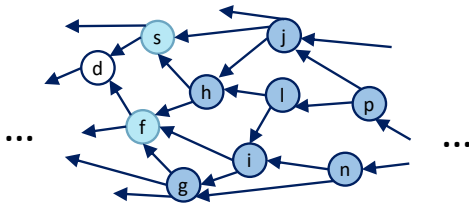


Figure 2: The darker blue nodes are all model nodes inheriting from the starting nodes n_s and n_f in lighter blue. A model node n_* corresponds to a model w_* .

3.3 UMIG-Assisted Unlearning

With an emphasis on knowledge inheritance and unlearning tasks, UMIG allows a model to retain and utilize previously learned useful information when receiving new data, achieving an effective combination of old and new knowledge. UMIG also allows the model to remove specific data for continuous optimization and performance improvement.

The UMIG-assisted unlearning consists primarily of the following two processes:

- **Locating unlearning subgraphs.** Based on the data that needs to be unlearned, a breadth-first search is conducted to identify the discovery nodes, which then spawn the subgraphs associated with the discovery nodes.
- **Updating models within unlearning subgraphs.** All model nodes, including discovery and inherited nodes within the identified unlearning subgraphs, are updated to unlearn the parts of their models affected by the data.

By performing a breadth-first search of the entire model network, one or more discovery nodes are identified based on unlearning requests related to specific data. These discovery nodes serve as the roots for the unlearning subgraphs. As depicted in Figure 2, the unlearning subgraphs may overlap since inherited nodes may inherit from multiple discovery nodes. For example, the discovery nodes, n_s and n_f , lead to two overlapping subgraphs with inherited nodes. Overlapping inherited nodes, such as n_h, n_j, n_l, n_p , would require the elimination of knowledge from multiple discovery nodes when unlearning due to their connections to different unlearning subgraphs. This situation is known as a **multi-root scenario**. In contrast, inherited nodes within one unlearning subgraph, such as n_g, n_i, n_n in a **single-root scenario**, only need to eliminate the impact from a single discovery node.

Inheritance is not just a simple mapping from the discovery nodes to the inherited nodes. Instead, it is achieved through multiple paths and varying depths. Each path represents a route of knowledge transfer via iteration, and the number of paths and differences in depth determine the complexity of the inheritance relationship.

A complex structure emerges when multiple paths are at varying depths from an inherited node to its corresponding discovery node(s), e.g., n_f, n_g, n_i or n_s, n_f, n_h, n_j . If unlearning operations are conducted simultaneously in terms of depth (in other words, nodes at the same depth from the root(s) are processed simultaneously and rely on sequential dependencies), nodes such as n_i and n_j may require multiple updates. This situation is termed an **imbalanced-path scenario**, contrasting with a **balanced-path scenario** (e.g., n_f, n_h, n_i, n_l), where each node requires only a single update due to uniform path lengths and synchronous processing at each depth. In cases where unlearning is conducted asynchronously, regardless of depth, both scenarios may require multiple updates.

Answer to RQ1: We propose the UMIG to effectively visualize model interdependence and capture the model inheritance in a structured way, leveraging the DAG structure. Assisted by UMIG, the models inheriting the knowledge to be removed can be rapidly identified. Moreover, the UMIG offers a systematic way to collect and prepare inheritance information, thus facilitating the unlearning process of inherited models. We also examine various learning frameworks of inherited models based on the numbers of their upstream models and the paths of knowledge inheritance to elucidate the emerging challenges and considerations of the unlearning process in inherited nodes due to model inheritance.

4 FIUN-BASED PARALLEL UNLEARNING

This section introduces a novel parallel unlearning method, Fisher Inheritance Unlearning (FIUn), designed to address the challenges associated with machine unlearning in large-scale UMIG model networks. A trusted learning network is considered where all learning contributors follow the designed unlearning process. The FIUn method operates under the general expression provided by the UMIG and leverages FIMs. It initiates the unlearning process by identifying specific model parameters that need updates, making the process more systematic. Derived from models in the unlearning graph, the training data, and the requested unlearning data, the FIMs are crucial in pinpointing essential model parameters and recommending their updated values.

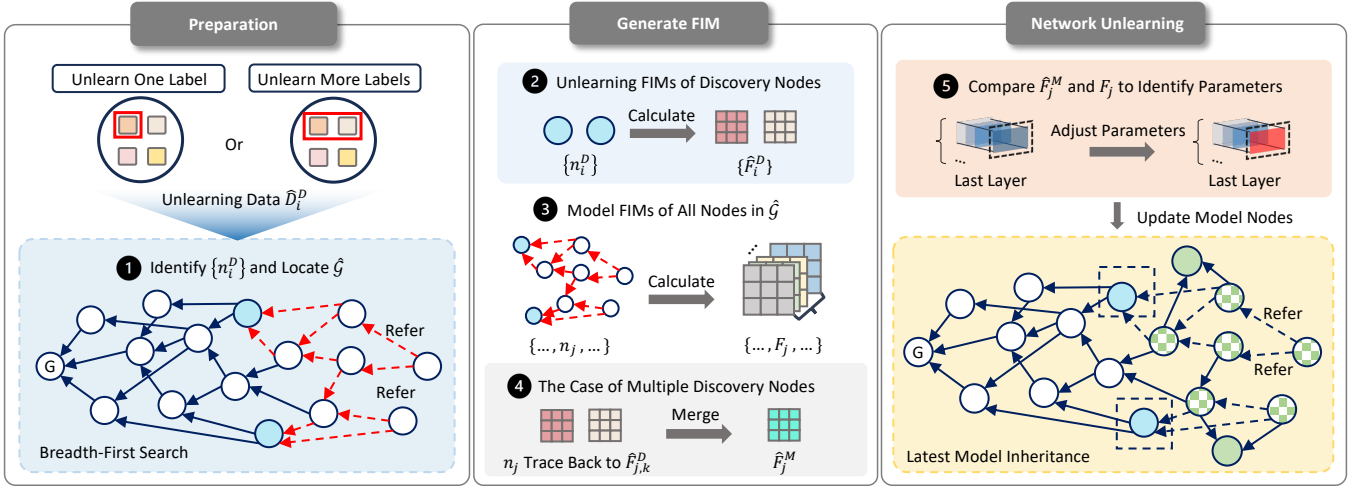


Figure 3: The unlearning process in \mathcal{G} consists of five steps: 1) Preparation. The discovery nodes $\{n_i^D\}$ are identified by performing a breadth-first search, with unlearning data \hat{D}_i^D containing one or more labels. Subsequently, the unlearning graph $\hat{\mathcal{G}}$ is located which root at $\{n_i^D\}$. 2) Calculate unlearning the unlearning FIMs $\{\hat{F}_i^D\}$ of $\{n_i^D\}$. 3) Calculate the model FIM F_j of node n_j in $\hat{\mathcal{G}}$. 4) Merge unlearning FIMs $\hat{F}_{j,k}^D$ for n_j in the case of multiple discovery nodes according to the topology. 5) Update n_j by comparing the merged unlearning FIM \hat{F}_j^M and F_j . Steps 2, 3, 4 and 5 apply to all nodes in $\hat{\mathcal{G}}$.

Algorithm 1: Fisher Inheritance Unlearning (FIUn)

- 1 **Input:** Model network $\mathcal{G} = (N, E)$, Unlearning task \mathcal{T}
 - 2 **Parameter:** γ, τ, η
 - 3 Use breadth-first search to identify discovery nodes $\{n_i^D\}$ and consequential unlearning graph $\hat{\mathcal{G}}$
 - 4 **for** n_i^D in $\{n_i^D\}$ **parallel do**
 - 5 Calculate unlearning FIM \hat{F}_i^D with Eq. (3)
 - 6 **end**
 - 7 **for** n_j in $\hat{\mathcal{G}}$ **parallel do**
 - 8 Calculate model FIM F_j with Eq. (4)
 - 9 Merge unlearning FIMs $\{\hat{F}_{j,k}^D\}$ with Eq. (5)
 - 10 Update model parameters of node n_j with Eq. (6)
 - 11 **end**
-

Notably, the FIUn method allows for the independent application of unlearning steps to each impacted model, facilitating a swift and effective parallel unlearning across extensive model networks. The FIUn method is depicted in Figure 3, and the procedural details are given in Algorithm 1.

4.1 Preparation

Upon receiving an unlearning task \mathcal{T} , accompanied by the unlearning dataset \hat{D} , FIUn initiates by conducting a breadth-first search from the starting node on the model network \mathcal{G} to identify the discovery nodes $\{n_i^D\}$. The discovery nodes are the first nodes exhibiting significant recognition of the unlearning data, with n_i^D representing the i -th discovery node. Subsequently, FIUn delineates

the unlearning graph $\hat{\mathcal{G}}$, which is rooted at the identified discovery nodes. FIUn then updates all nodes in the unlearning graph to unlearn the requested unlearning knowledge.

4.2 FIUn

The main idea of FIUn is to identify critical model parameters by comparing the FIM from the unlearning dataset with the FIM from the training dataset. The differences between these matrices highlight the necessary adjustments in model parameters to achieve effective unlearning. The FIUn process unfolds as follows.

4.2.1 Calculate unlearning FIMs of discovery nodes. The FIUn method initiates by assessing the impact of the unlearning data on the model parameters of the discovery nodes, utilizing the FIM as specified in Eq. (3). This assessment is conducted using the model parameters and the unlearning data (see line 5, Algorithm 1).

The unlearning FIM for the i -th identified discovery node, n_i^D , is denoted by \hat{F}_i^D and is calculated as

$$\hat{F}_i^D = \mathbb{E} \left[\left(\frac{\partial \ln p(\hat{D}_i^D | w_i^t)}{\partial w_i^t} \right) \left(\frac{\partial \ln p(\hat{D}_i^D | w_i^t)}{\partial w_i^t} \right)^\top \right]_{w_{\hat{D}_i^D}^*}, \quad (3)$$

where \hat{D}_i^D represents the unlearning data for n_i^D , w_i^t denotes the last layer parameters of the model w_i at node n_i^D , and $w_{\hat{D}_i^D}^*$ refers to the optimal parameters learned on \hat{D}_i^D .

The unlearning FIM highlights the importance of each parameter in the last layer with respect to the specific unlearning task [29, 64]. In FIUn, the FIM calculation is restricted to the last layer parameters while other layers remain frozen, aimed at reducing the computational complexity associated with FIM calculations, which is a challenge in traditional FIM-based unlearning methods.

Using the last layer for unlearning can focus on the most relevant features. Since the last layer directly affects the final decision of the model, adjusting its parameters can effectively facilitate unlearning goals while maintaining stable performance on data not subject to unlearning [22].

4.2.2 Calculate model FIMs of all nodes in unlearning graph. The FIUn method proceeds by calculating the model FIMs of all models within the unlearning graph to identify the impact of model parameters in each node (see line 8, Algorithm 1).

For the j -th node n_j in the unlearning graph $\hat{\mathcal{G}}$, either a discovery node or an inherited node, the model FIM, denoted by F_j , is given by

$$F_j = \mathbb{E} \left[\left(\frac{\partial \ln p(D_j | w_j^L)}{\partial w_j^L} \left(\frac{\partial \ln p(D_j | w_j^L)}{\partial w_j^L} \right)^\top \right) \right]_{w_{D_j}^*}, \quad (4)$$

where D_j is the training data for n_j , w_j^L denotes the last layer parameters of the model w_j at node n_j , and $w_{D_j}^*$ denotes the optimal parameters learned on D_j .

The model FIM quantifies the knowledge about the training dataset embedded in the model parameters and highlights the significance of each parameter. Similar to the unlearning FIM, only the FIM for the last layer parameter is calculated, aiming to minimize computational complexity.

4.2.3 Merge unlearning FIMs for all nodes in the unlearning graph. The FIUn method estimates the unlearning FIM for all nodes within the unlearning graph, including both discovery and inherited nodes (see line 9, Algorithm 1). The unlearning FIMs from discovery nodes are merged to form a collective unlearning FIM for each node in the unlearning graph. This merger is crucial as the linkages between the unlearning data and parameters are embedded within the model and can persist through model inheritance [13], especially in multi-root scenarios where an inherited node may trace back to several discovery nodes. A novel merging FIM function is introduced, denoted by $\Phi(\cdot)$, and is defined as

$$\hat{F}_j^M = \Phi \left(\{ \hat{F}_{j,k}^D \} \right), \quad (5)$$

where \hat{F}_j^M is the merged unlearning FIM for the j -th node in the unlearning graph, the set $\{ \hat{F}_{j,k}^D \}$ collects the unlearning FIMs of discovery nodes within $\hat{\mathcal{G}}$ that can be traced back from node n_j , and k denotes the k -th discovery node reachable from n_j . In this paper, the element-wise maximum is employed for the merging FIM function. Specifically, \hat{F}_j^M assembles the largest elements among the unlearning FIMs of discovery nodes in multi-root scenarios and takes the only unlearning FIM in single-root scenarios.

As shown in Figure 4, the model w_h inherits from models w_j , w_s , and w_f and needs to remove all requested unlearning data, though each discovery node contains only a portion of the unlearning data. The FIM of each model reflects the sensitivity of its parameters to the unlearning data, which can be interpreted as parameter importance. By taking the maximum of the corresponding elements across these unlearning FIMs, the merged FIM encompasses all unlearning tasks from the discovery nodes and effectively identifies the parameters that need updating to achieve complete unlearning.

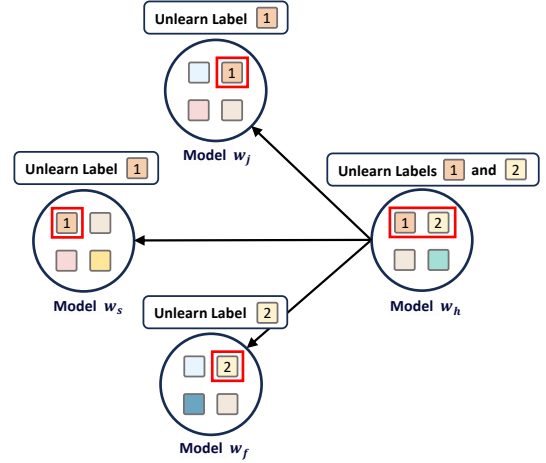


Figure 4: There are three discovery nodes that need to undergo the unlearning process, namely model w_j , model w_s and model w_f . The labels to be unlearned are label 1 and label 2. However, model w_j and model w_s only have label 1, while model w_f only has label 2. Model w_h inherits from these three discovery nodes, so we merge the unlearning FIMs of the discovery nodes and perform the unlearning of label 1 and label 2 on model w_h together.

4.2.4 Update models in unlearning graph. In the final step, the FIUn method identifies which parameters need to be updated by comparing the merged FIM with the model FIM, as described in line 10 of Algorithm 1. The outcomes of this comparison are also utilized to scale the parameters. For node n_j in the unlearning graph, the parameters are updated as

$$\hat{w}_{j,l}^L = \begin{cases} \min(\tau \frac{F_{j,l}}{\hat{F}_{j,l}^M}, \eta) w_{j,l}^L, & \text{if } \frac{\hat{F}_{j,l}^M}{F_{j,l}} > \gamma; \\ w_{j,l}^L, & \text{if } \frac{\hat{F}_{j,l}^M}{F_{j,l}} \leq \gamma, \end{cases} \quad (6)$$

where $w_{j,l}^L$ and $\hat{w}_{j,l}^L$ are the l -th parameter in the last layer before and after the unlearning update, respectively. Similarly, $F_{j,l}$ and $\hat{F}_{j,l}^M$ are the l -th element of the model FIM and merged unlearning FIM of node n_j , respectively. The hyperparameters, including τ , η , and γ , balance the unlearning impact on the unlearning data and the accuracy of the retained data.

During the model updating phase, only the parameters of the last layer are updated while the other layers remain frozen, consistent with our design of the unlearning FIM and model FIM, where only the FIM of the last layer is calculated. Elements within the FIM indicate the significance of each parameter relative to the dataset. The threshold γ identifies the critical parameters that are significant for the unlearning task, and these parameters are scaled down accordingly. The hyperparameter η ensures minimal change to achieve the desired unlearning effect. Non-critical parameters are left unchanged to maintain accuracy on data that does not require unlearning.

4.3 Discussion

From the perspective of the FIM, the impact of data on specific model parameters is consistently localized at precise positions

within the parameter space [13]. The stable localization of the FIM across iterations helps precisely locate the parameter locations for unlearning at the class, client, and sample levels using data tied to specific label sets. By fine-tuning τ , η , and γ in Eq. (6) to match the sample size of the class being unlearned, the task transits flexibly between the class-level [13] and sample-level unlearning [16]. Specifically, when the unlearning FIM mirrors the model’s FIM with a class-level setting, it becomes a client-level unlearning task. All types of unlearning are performed irrespective of the succession of inheritance relationships. Consequently, employing FIUn disrupts the sequential dependencies traditionally required for unlearning, thus enabling fully parallel unlearning processes across any number of subgraphs.

Not only can models across different subgraphs undergo parallel unlearning, but those within the same subgraph at various depths can also be unlearned in parallel, thanks to a feature referred to as *Hyper-Distance* in this paper. This *Hyper-Distance* is achieved without compromising the integrity of the inheritance relationships. *Hyper-Distance* ensures that both unlearned and retained knowledge is effectively managed along the inheritance paths. This efficiency is possible because the FIUn method utilizes FIMs for unlearning, enabling a class-wise inheritance approach. Each model effectively incorporates a union of label sets from its predecessors, ensuring that the inheritance is preserved. Simultaneously, by focusing on label differences, we achieve fully parallel unlearning—making depths and paths irrelevant to the process.

Answer to RQ2: The FIUn method enables independently removing knowledge from each inherited model. This method utilizes the FIM to obtain the *Hyper-Distance* property which breaks sequential dependencies among models, enabling fully parallel unlearning on inherited models and significantly decreasing the execution time of unlearning tasks. To address the complexity arising from multiple upstream models, the merging FIM function is developed to aggregate unlearning FIMs from those models, facilitating the efficient, one-shot removal of inherited knowledge.

We also map the FIUn method and merging FIM function to the UMIG-assisted unlearning scenarios described in Section 3.3. This demonstrates how the proposed approach efficiently facilitates unlearning through the property of *Hyper-Distance*. **Converting Imbalance into Balance.** This scenario is particularly significant due to the fact that existing unlearning methods suffer from inevitable sequential dependencies. FIUn leverages the *Hyper-Distance* property to circumvent the influences of depths and paths within the inheritance topology. Consequently, imbalanced-path scenarios can be managed as effectively as balanced-path scenarios, where only one update operation is needed, regardless of whether unlearning is conducted synchronously or asynchronously, i.e., only one unlearning FIM needs to be computed for each inherited node.

Converting Multi-root into Single-root. The merging FIM function is proposed to refine multi-root scenarios. This function merges the FIMs of the corresponding unlearned label sets from multiple discovery nodes into a single FIM, as shown in Figure 4. Specifically, overlapping inherited nodes require only one update operation to eliminate the impact of multiple discovery nodes by conducting a parameter-wise merger, where only the most impactful parameters

take effect in this FIM. This function eliminates the need for multiple comparisons among various unlearning FIMs in multi-root scenarios, hence enhancing unlearning efficiency.

4.4 Implementation

4.4.1 System Setting. In practice, FIUn can be handled differently depending on the system architecture, as described in the following:

- *Centralized:* Model FIMs are computed and attached along with the model being published and sent to the central coordinator. When an unlearning request is initiated, the central server performs unlearning by merging the unlearning FIMs of the discovery nodes and executes unlearning in parallel.
- *Decentralized:* The discovery nodes publicly share Each unlearning FIM. Owners of each inherited node can then combine these unlearning FIMs with their own local models at will, according to specific unlearning requirements. This decentralized approach enables efficient and effective unlearning.

4.4.2 Complexity. The computational complexity of an unlearning task comprises the complexities of Steps 1, 3, and 4 (i.e., calculate unlearning FIM, merge unlearning FIMs and update models). The complexity of Step 2 is not considered, as the computation of the model FIM can be performed beforehand. The overall complexity for the unlearning task is $O(|\hat{D}||L| + |\{n_i^p\}| + |L|)$. Breaking down the complexities, Eq. (3) and Eq. (4) update $|L|$ parameters per data entry, with complexities $O(|\hat{D}_i^p||L|)$ and $O(|D_j||L|)$, respectively, where $|\hat{D}_i^p| \leq |\hat{D}|$ and $|L|$ is the number of parameters in the last layer. The term $O(|D_j||L|)$ is omitted as model FIMs can be calculated along with the model training prior to any unlearning tasks. Eq. (5) includes a comparison and merger of K unlearning FIMs, leading to a complexity of $O(K)$, where K is the number of traceable discovery nodes in the unlearning graph \hat{G} from node n_j and $K \leq |\{n_i^p\}|$. Eq. (6) updates $|L|$ model parameters, leading to a complexity of $O(|L|)$. As the computation of the unlearning FIM for discovery nodes and the model updates can proceed in parallel, the overall complexity of the unlearning tasks is $O(|\hat{D}||L| + |\{n_i^p\}| + |L|)$.

5 EXPERIMENTAL SETTINGS

This section first presents the datasets used in the experiments, the models selected, and the performance metrics for accuracy evaluation, followed by the topology setups and the benchmarks for unlearning to evaluate the FIUn method.

5.1 Datasets and Models

Datasets. The experiment uses two datasets to evaluate the proposed FIUn method. These two datasets are benchmarks for image classification tasks, encompassing diverse image classification tasks.

- **CIFAR100 [27].** This dataset consists of 60,000 color images in 100 classes, with 600 images per class. The images are of size 32×32 pixels. The dataset is divided into 50,000 training images and 10,000 test images. Each class in the CIFAR-100 dataset belongs to one of 20 superclasses. There is a coarse label (superclass) and a fine label (specific class) per image.

Table 1: Baseline of Federated Unlearning Performance On CIFAR-100 Unlearning Speed Comparison

Model	# C_f	Cumulative Unlearning Time (s)														
		Gradient ascent			Finetune			Distill			Re-training			FIUn		
		w_g	w_a	w_b	w_g	w_a	w_b	w_g	w_a	w_b	w_g	w_a	w_b	w_g	w_a	w_b
AlexNet	1	0.97	1.05	1.26	0.54	0.75	1.08	82.5	153.65	294.32	29.70	59.06	89.62	0.09	0.11	0.13
	2	0.99	1.17	1.39	0.57	0.77	1.15	80.49	155.63	315.52	28.69	57.81	84.97	0.11	0.16	0.13
	10	1.1	1.27	1.68	0.53	1.95	2.31	75.3	147.6	326.8	21.96	42.37	63.82	0.11	0.14	0.15
ResNet18	1	2.45	2.89	3.42	0.74	1.32	1.74	70.31	129.44	247.6	30.36	61.40	90.94	0.68	1.00	0.99
	2	2.02	2.2	2.78	0.76	1.22	1.79	76.55	139.55	259.53	28.30	57.39	84.06	0.69	1.03	1.09
	10	2.02	2.58	3.67	0.85	1.54	1.84	75.12	150.35	267.34	22.03	44.83	66.30	0.76	1.14	1.04

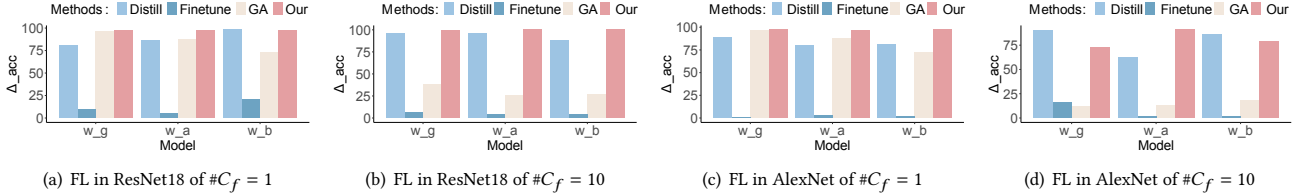


Figure 5: Baseline of Federated Unlearning Performance On CIFAR-100.

- **TinyImageNet [28].** This dataset contains 200 classes, each with 500 training images, 50 validation images, and 50 test images, with a total of up to 100,000 images. The images are resized to 64×64 pixels, making them smaller than those in the original ImageNet dataset but larger than those in CIFAR-100.

Models. We use the AlexNet model [20], ResNet18 model [43] and DenseNet161 model [52] to evaluate the impact of our proposed FIUn method on the accuracy of the unlearned label set C_f and the retained label set C_r .

Performance Metrics. We use the training datasets to check the accuracy of the model to evaluate its practicality in experiments. This is a common and reasonable approach since it directly evaluates if the removed information still influences the model, as widely accepted in the field [16, 22, 53].

- **Accuracy on unlearned labels (AD_f).** The accuracy of the unlearned label set in the unlearning model ideally would be close to zero. We use the training datasets to test the effectiveness of unlearning.
- **Accuracy on retained labels (AD_r).** The accuracy of a retained label set of the unlearning model. It is expected to be close to the accuracy of the original model before unlearning.
- **Cumulative unlearning time.** The cumulative time required for each model to unlearn labels during the training process in machine learning and deep learning.
- **Accuracy difference index (Δ_{acc}).** The difference between AD_r and AD_f also serves as a direct metric to evaluate unlearning

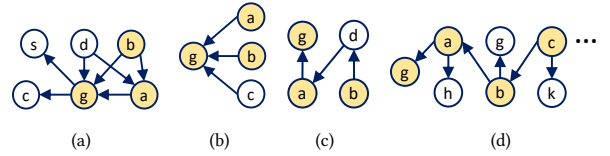


Figure 6: Models topologies considered in the experiments.

performance. The greater the difference, the more effective the unlearning is, with a maximum 1.

5.2 Learning Framework Setup and Benchmarks

Targeted Frameworks. We detailed setups for four learning frameworks under the UMIG with varying dataset and label distribution conditions.

- **Federated Unlearning.** This process uses the structure shown in Figure 6(a). The CIFAR100 and TinyImageNet datasets are each randomly divided into five parts. When the model w_g contains labels that need to be unlearned, the models that inherit from it need to perform the unlearning operation. We select models w_g , w_a , and w_b for experimental demonstration.
- **Distributed Data-Parallel Unlearning.** This process uses the structure shown in Figure 6(b). The CIFAR100 and TinyImageNet datasets are each randomly divided into three parts, each executing a sub-task in parallel. When the model w_g contains labels

Table 2: Federated Unlearning Performance On TinyImageNet

Model	# C_f	Metrics	Original Model (%)			Re-training Model (%)			FIUn (%)			Cumulative Unlearning Time (s)					
			w_g	w_a	w_b	w_g	w_a	w_b	w_g	w_a	w_b	Re-training			FIUn		
DenseNet161	1	$AD_r \uparrow$	99.99	99.99	99.81	99.99	99.99	98.80	88.03	77.64	76.02	999.41	1996.43	2997.64	2.51	4.59	4.95
		$AD_f \downarrow$	99.99	99.99	99.66	0.00	0.00	0.00	0.00	0.00	0.00						
	4	$AD_r \uparrow$	99.99	99.99	99.80	99.99	99.99	99.51	83.01	71.43	71.00	1004.64	2006.31	3006.14	3.16	4.69	4.89
		$AD_f \downarrow$	99.99	99.99	99.49	0.00	0.00	0.00	0.00	0.00	0.00						
	6	$AD_r \uparrow$	99.99	99.99	99.96	99.99	99.99	99.16	80.00	67.67	66.58	1019.43	2020.16	3018.64	3.10	4.96	4.75
		$AD_f \downarrow$	99.99	99.99	99.89	0.00	0.00	0.00	0.00	0.00	0.00						
	10	$AD_r \uparrow$	99.99	99.99	99.72	99.71	99.99	99.99	71.68	58.01	55.80	1031.43	2029.64	3030.64	2.95	4.85	4.89
		$AD_f \downarrow$	99.99	99.99	98.82	0.00	0.00	0.00	0.00	0.00	0.00						
ResNet18	1	$AD_r \uparrow$	99.99	99.99	99.99	99.99	99.99	99.99	99.73	99.97	99.46	112.95	216.39	314.29	1.35	3.68	3.42
		$AD_f \downarrow$	99.99	99.99	99.99	0.00	0.00	0.00	0.00	0.00	0.00						
	4	$AD_r \uparrow$	99.99	99.99	99.99	99.99	99.99	99.99	99.17	99.98	99.98	109.89	209.31	310.42	1.63	3.26	3.57
		$AD_f \downarrow$	99.99	99.99	99.99	0.00	0.00	0.00	0.00	0.00	0.00						
	6	$AD_r \uparrow$	99.99	99.99	99.99	99.96	99.99	99.99	99.54	99.98	99.98	107.39	208.12	305.32	1.46	3.37	3.51
		$AD_f \downarrow$	99.99	99.99	99.99	0.00	0.00	0.00	0.00	0.00	0.00						
	10	$AD_r \uparrow$	99.99	99.99	99.99	99.99	99.99	99.99	99.98	99.99	99.99	104.21	201.36	302.74	1.52	3.21	3.36
		$AD_f \downarrow$	99.99	99.99	99.99	0.00	0.00	0.00	0.00	0.00	0.00						

Table 3: Incremental Unlearning Performance On TinyImageNet

Model	# C_f	Metrics	Original Model (%)			Re-training Model (%)			FIUn (%)			Cumulative Unlearning Time (s)					
			w_g	w_a	w_b	w_g	w_a	w_b	w_g	w_a	w_b	w_g	w_a	w_b	w_g	w_a	w_b
DenseNet161	1	$AD_r \uparrow$	99.99	99.99	99.81	99.99	99.99	98.80	89.76	78.50	73.87	991.43	1995.36	3989.47	2.75	4.85	4.43
		$AD_f \downarrow$	99.99	99.99	99.66	0.00	0.00	0.00	0.00	0.00	0.00						
	4	$AD_r \uparrow$	99.99	99.99	99.80	99.99	99.99	99.51	83.98	65.87	59.11	1006.32	2004.75	4009.41	2.64	4.43	4.64
		$AD_f \downarrow$	99.99	99.99	99.49	0.00	0.00	0.00	0.00	0.00	0.00						
	6	$AD_r \uparrow$	99.99	99.99	99.96	99.99	99.99	99.16	86.81	61.02	55.04	1019.43	2019.50	4019.46	2.36	4.47	4.74
		$AD_f \downarrow$	99.99	99.99	99.89	0.00	0.00	0.00	0.00	0.00	0.00						
	10	$AD_r \uparrow$	99.99	99.99	99.72	99.99	99.99	99.99	85.95	54.61	45.46	1035.36	2041.78	4039.75	2.65	4.46	4.75
		$AD_f \downarrow$	99.99	99.99	99.99	0.00	0.00	0.00	0.00	0.00	0.00						
ResNet18	1	$AD_r \uparrow$	99.99	99.99	99.99	99.99	99.99	99.99	98.66	96.33	96.07	120.32	221.75	439.85	1.37	3.75	3.43
		$AD_f \downarrow$	99.99	99.99	99.99	0.00	0.00	0.00	0.00	0.00	0.00						
	4	$AD_r \uparrow$	99.99	99.99	99.99	99.99	99.99	99.99	98.84	96.34	96.70	115.32	217.33	435.17	1.41	3.34	3.64
		$AD_f \downarrow$	99.99	99.99	99.99	0.00	0.00	0.00	0.00	0.00	0.00						
	6	$AD_r \uparrow$	99.99	99.99	99.99	99.96	99.99	99.99	98.82	99.99	98.59	110.32	211.35	431.37	1.47	3.46	3.75
		$AD_f \downarrow$	99.99	99.99	99.99	0.00	0.00	0.00	0.00	0.00	0.00						
	10	$AD_r \uparrow$	99.99	99.99	99.99	99.99	99.99	99.99	99.33	97.51	98.45	108.32	207.43	428.43	1.32	3.56	3.57
		$AD_f \downarrow$	99.99	99.99	99.99	0.00	0.00	0.00	0.00	0.00	0.00						

that need to be unlearned, each sub-task performs the unlearning operation in parallel. We select models w_g , w_a , and w_b for experimental demonstration.

- **Incremental Unlearning.** This process uses the structure shown in Figure 6(c). In the CIFAR100 dataset, the first model is trained on data with labels 0-90, and each inheriting model's training dataset progressively includes two additional classes. In the TinyImageNet dataset, the first model is trained on data with labels 0-190, and similarly, each inheriting model's training dataset progressively includes two additional classes. We select models w_g , w_a , and w_b for experimental demonstration.
- **Transfer Unlearning.** Since TL involves fine-tuning the last layer parameters, adjustments are focused on the last layer of the model. Experiments, as illustrated in Figure 6(b), involve the CIFAR100 dataset where a model w_g is trained on labels 0-90 and then transferred to models w_a and w_b trained on labels 0-92 and

0-98, respectively. Similarly, for the TinyImageNet dataset, model w_g is trained on labels 0-190 and then transferred to models w_a and w_b , which are trained on labels 0-192 and 0-198, respectively.

Benchmark. The experiment specifically focuses on class-level unlearning tasks for clarity of presentation. We re-train the models that include unlearned labels and subsequent models influenced by these labels due to inheritance. We remove the data with unlearned labels from each model's dataset. The remaining data is then used to individually train each model. The models are trained sequentially according to their inheritance relationships.

Hyperparameters. The hyperparameters used in the experiment are shown in **Appendix .1**. The table lists the learning rates, optimizers, and other hyperparameters for different models, as well as the hyperparameters of our proposed FIUn method. Throughout the experimental process, all the hyperparameters remain unchanged to ensure a fair comparison of our method among different models.

Table 4: Transfer Unlearning Performance On CIFAR-100

Model	# C_f	Metrics	Original Model (%)			Re-training Model (%)			FIUn (%)			Cumulative Unlearning Time (s)					
												Re-training			FIUn		
			w_g	w_a	w_b	w_g	w_a	w_b	w_g	w_a	w_b	w_g	w_a	w_b	w_g	w_a	w_b
AlexNet	1	$AD_r \uparrow$	97.16	95.61	92.20	98.17	95.98	91.32	91.40	86.24	83.99	20.31	40.49	42.36	0.09	0.11	0.11
		$AD_f \downarrow$	96.66	99.99	99.99	0.00	0.00	0.00	0.00	0.00	0.00						
	2	$AD_r \uparrow$	97.16	95.61	92.20	96.88	96.68	93.16	82.36	80.47	79.99	21.20	40.56	41.92	0.08	0.13	0.11
		$AD_f \downarrow$	99.99	99.99	99.99	0.00	0.00	0.00	0.00	0.00	0.00						
	4	$AD_r \uparrow$	97.16	95.61	92.20	94.67	96.45	93.45	71.59	71.43	76.06	20.30	39.76	40.60	0.09	0.11	0.11
		$AD_f \downarrow$	96.61	98.30	98.30	0.00	0.00	0.00	0.00	0.00	0.00						
	10	$AD_r \uparrow$	97.16	95.61	92.20	99.99	99.99	99.99	75.97	69.56	76.15	19.42	39.46	39.35	0.08	0.13	0.11
		$AD_f \downarrow$	98.57	99.28	99.28	0.00	0.00	0.00	20.28	20.28	20.28						
ResNet18	1	$AD_r \uparrow$	99.99	99.99	99.99	99.99	99.99	99.99	89.09	93.51	95.22	22.21	41.52	42.93	0.15	0.24	0.24
		$AD_f \downarrow$	99.99	99.99	99.99	0.00	0.00	0.00	0.00	0.00	0.00						
	2	$AD_r \uparrow$	99.99	99.99	99.99	99.99	99.99	99.99	85.89	94.89	95.79	21.19	41.72	43.20	0.17	0.23	0.26
		$AD_f \downarrow$	99.99	99.99	99.99	0.00	0.00	0.00	0.00	0.00	0.00						
	4	$AD_r \uparrow$	99.96	99.99	99.99	99.99	99.99	99.99	80.20	94.82	97.03	22.03	42.26	43.25	0.17	0.25	0.25
		$AD_f \downarrow$	99.99	99.99	99.99	0.00	0.00	0.00	0.00	0.00	0.00						
	10	$AD_r \uparrow$	99.96	99.99	99.99	99.99	99.99	99.99	75.36	98.07	98.96	19.10	42.60	41.36	0.16	0.27	0.27
		$AD_f \downarrow$	99.99	99.99	99.99	0.00	0.00	0.00	0.00	0.00	0.00						

Table 5: Distributed Data-Parallel Unlearning Performance On CIFAR-100

Model	# C_f	Metrics	Original Model (%)			Re-training Model (%)			FIUn (%)			Cumulative Unlearning Time (s)					
												Re-training			FIUn		
			w_g	w_a	w_b	w_g	w_a	w_b	w_g	w_a	w_b	w_g	w_a	w_b	w_g	w_a	w_b
AlexNet	1	$AD_r \uparrow$	98.01	99.96	99.96	99.96	99.96	99.96	97.23	98.85	97.66	30.13	31.26	31.14	0.09	0.14	0.23
		$AD_f \downarrow$	99.99	99.96	99.96	0.00	0.00	0.00	0.00	0.00	0.00						
	2	$AD_r \uparrow$	99.96	99.96	99.96	99.96	99.96	99.96	96.14	97.07	96.71	26.43	26.47	26.41	0.11	0.16	0.27
		$AD_f \downarrow$	99.96	99.96	99.96	0.00	0.00	0.00	0.00	0.00	0.00						
	4	$AD_r \uparrow$	98.01	99.96	99.96	99.96	99.96	99.96	94.58	90.41	90.97	24.33	24.36	24.37	0.10	0.14	0.23
		$AD_f \downarrow$	99.09	99.96	99.96	0.00	0.00	0.00	0.00	0.00	0.00						
	10	$AD_r \uparrow$	98.01	99.96	99.96	99.96	99.96	99.96	91.53	76.19	80.70	21.03	22.96	22.10	0.10	0.14	0.24
		$AD_f \downarrow$	97.15	99.96	99.96	0.00	0.00	0.00	9.73	0.00	11.08						
ResNet18	1	$AD_r \uparrow$	99.99	99.99	99.99	99.99	99.99	99.99	91.87	94.67	93.67	32.53	31.95	32.18	0.30	0.34	0.64
		$AD_f \downarrow$	99.99	99.99	99.99	0.00	0.00	0.00	0.00	0.00	0.00						
	2	$AD_r \uparrow$	99.99	99.99	99.99	99.99	99.99	99.99	89.94	94.58	92.40	28.28	27.22	28.47	0.30	0.34	0.66
		$AD_f \downarrow$	99.99	99.99	99.99	0.00	0.00	0.00	0.00	0.00	0.00						
	4	$AD_r \uparrow$	99.96	89.20	88.52	99.96	99.96	86.44	93.95	89.26	91.77	25.37	24.97	25.13	0.31	0.35	0.66
		$AD_f \downarrow$	99.99	99.99	99.99	0.00	0.00	0.00	0.00	0.00	0.00						
	10	$AD_r \uparrow$	99.96	89.20	88.52	99.96	99.96	99.96	90.44	95.79	94.19	22.60	21.92	24.19	0.34	0.34	0.68
		$AD_f \downarrow$	99.99	99.99	99.99	0.00	0.00	0.00	9.73	0.00	0.00						

5.3 Label Category Settings

The unlearned label categories are represented as $\#C_f$. The distribution of labels among different models may also vary in different data distributions. For instance, model w_a aims to unlearn labels 1, 2, 3, and 4, while model w_b intends to unlearn labels 2, 3, 5, and 6. In this case, there is an overlap between the unlearned label categories of model w_a and model w_b , specifically labels 2 and 3. We refer to the degree of overlapping among these unlearned label categories as $\#\cap_f$.

The unlearning process is applied to individual categories and various combinations of labels. For the CIFAR-100 dataset, the combinations we select include 1, 2, 4, and 10 categories. For the Tiny-ImageNet dataset, the selected combinations include 1, 4, 6, and 10

categories. The overlap of the unlearned label categories is divided into different proportions, including 60%, 40%, 20%, and 0%.

6 EVALUATION

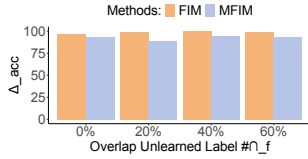
In this section, we use NVIDIA 4090 GPU to set up a test platform that demonstrates the impact of the FIUn method on the accuracy of unlearned and retained labels in four frameworks: FL, DDPL, IL and TL. When assessing accuracy and time consumption across these learning frameworks during the model unlearning process, we compare our proposed FIUn method with existing unlearning methods and use re-training as a benchmark. We also analyze the impact of the inheritance depth and parameter layers of the models on unlearning effectiveness.

Table 6: Federated Unlearning Performance On TinyImageNet With Multiple Label Distribution

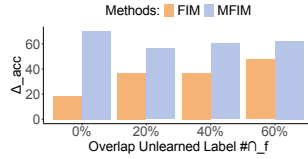
Model	# \cap_f	Metrics	Original Model (%)			Re-training Model (%)			FIUn (%)			Cumulative Unlearning Time (s)					
			w_g	w_a	w_b	w_g	w_a	w_b	w_g	w_a	w_b	Re-training			FIUn		
												w_g	w_a	w_b	w_g	w_a	w_b
DenseNet161	60%	$AD_r \uparrow$	99.99	99.99	99.81	98.80	99.99	99.99	96.39	84.75	77.89	3000.66	1998.46	994.32	4.69	2.39	2.30
		$AD_f \downarrow$	99.99	99.99	99.66	0.00	0.00	0.00	0.00	0.00	0.00						
	40%	$AD_r \uparrow$	99.50	99.99	99.80	99.51	99.99	99.99	96.64	85.40	85.00	3009.53	1010.45	2011.14	5.12	2.69	2.14
		$AD_f \downarrow$	99.99	99.99	99.49	0.00	0.00	0.00	0.00	0.00	0.00						
	20%	$AD_r \uparrow$	99.99	99.99	99.96	99.16	99.99	99.99	96.22	81.49	78.83	3022.64	2020.67	1021.34	4.98	2.64	2.59
		$AD_f \downarrow$	99.99	99.99	99.89	0.00	0.00	0.00	0.00	0.00	0.00						
	0%	$AD_r \uparrow$	99.99	99.99	99.99	99.99	99.99	99.71	96.01	83.04	79.15	3039.64	2041.32	1046.14	4.96	2.14	2.50
		$AD_f \downarrow$	99.99	99.99	98.82	0.00	0.00	0.00	0.00	0.00	0.00						
ResNet18	60%	$AD_r \uparrow$	99.99	99.99	99.99	99.99	99.99	99.99	95.23	98.54	98.44	349.32	246.43	123.74	3.16	1.65	1.68
		$AD_f \downarrow$	99.99	99.99	99.99	0.00	0.00	0.00	0.00	0.00	0.00						
	40%	$AD_r \uparrow$	99.99	99.99	99.99	99.99	99.99	99.99	96.98	99.44	99.49	355.32	247.64	128.43	2.97	1.46	1.59
		$AD_f \downarrow$	99.99	99.99	99.99	0.00	0.00	0.00	0.00	0.00	0.00						
	20%	$AD_r \uparrow$	99.99	99.99	99.99	99.96	99.99	99.99	94.43	98.86	99.38	354.83	246.43	129.35	2.89	1.54	1.38
		$AD_f \downarrow$	99.99	99.99	99.99	0.00	0.00	0.00	0.00	0.00	0.00						
	0%	$AD_r \uparrow$	99.99	99.99	99.99	99.99	99.99	99.99	97.36	99.34	99.32	351.38	244.34	125.32	3.10	1.69	1.39
		$AD_f \downarrow$	99.99	99.99	99.99	0.00	0.00	0.00	0.00	0.00	0.00						

Table 7: Distributed Data-Parallel Unlearning Performance On CIFAR-100 With Multiple Label Distribution

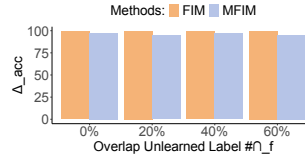
Model	# \cap_f	Metrics	Original Model (%)			Re-training Model (%)			FIUn (%)			Cumulative Unlearning Time (s)					
			w_g	w_a	w_b	w_g	w_a	w_b	w_g	w_a	w_b	Re-training			FIUn		
												w_g	w_a	w_b	w_g	w_a	w_b
DenseNet161	60%	$AD_r \uparrow$	99.99	99.99	99.81	98.80	99.99	99.99	95.18	97.07	99.99	999.41	996.43	997.64	0.15	0.08	0.09
		$AD_f \downarrow$	99.99	99.99	99.66	0.00	0.00	0.00	0.00	0.00	0.00						
	40%	$AD_r \uparrow$	99.99	99.99	99.80	99.51	99.99	99.99	90.53	97.07	98.82	1004.64	1006.31	1006.14	0.19	0.09	0.11
		$AD_f \downarrow$	99.99	99.99	99.49	0.00	0.00	0.00	0.00	0.00	0.00						
	20%	$AD_r \uparrow$	99.99	99.99	99.96	99.16	99.99	99.99	95.29	97.07	99.89	1019.43	1020.16	1018.64	0.18	0.07	0.10
		$AD_f \downarrow$	99.99	99.99	99.89	0.00	0.00	0.00	0.00	0.00	0.00						
	0%	$AD_r \uparrow$	99.99	99.99	99.99	99.99	99.99	99.99	87.15	97.07	96.36	1031.43	1029.64	1030.64	0.18	0.10	0.11
		$AD_f \downarrow$	99.99	99.99	98.82	0.00	0.00	0.00	0.00	0.00	0.00						
ResNet18	60%	$AD_r \uparrow$	99.99	99.99	99.99	99.99	99.99	99.99	97.62	88.94	87.87	30.36	33.18	37.31	0.60	0.32	0.29
		$AD_f \downarrow$	99.99	99.99	99.99	0.00	0.00	0.00	0.00	0.00	0.00						
	40%	$AD_r \uparrow$	99.99	99.99	99.99	99.99	99.99	99.99	96.50	89.35	87.89	28.30	29.13	52.33	0.59	0.34	0.30
		$AD_f \downarrow$	99.99	99.99	99.99	0.00	0.00	0.00	0.00	0.00	0.00						
	20%	$AD_r \uparrow$	99.99	99.99	99.99	99.96	99.99	99.99	95.31	88.17	93.06	26.39	23.37	56.61	0.58	0.28	0.30
		$AD_f \downarrow$	99.99	99.99	99.99	0.00	0.00	0.00	0.00	0.00	0.00						
	0%	$AD_r \uparrow$	99.99	99.99	99.99	99.99	99.99	99.99	88.87	88.86	89.16	22.03	24.36	46.42	0.64	0.37	0.32
		$AD_f \downarrow$	99.99	99.99	99.99	0.00	0.00	0.00	0.00	0.00	0.00						



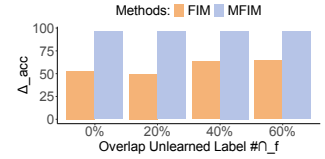
(a) FL in CIFAR100 ResNet18



(b) FL CIFAR100 by AlexNet



(c) FL TinyImageNet by ResNet18



(d) FL TinyImageNet by DenseNet161

Figure 7: Overlap $\# \cap_f$ analysis, $\# C_f = 15$.

6.1 General Label Unlearning Analysis

We consider existing emerging unlearning methods for comparison: 1) Fine-tuning, which adjusts the original model using the remaining dataset [43], 2) Gradient ascent (GA), employing negative gradients for unlearning [65], and 3) Distill, which distills

knowledge from the original model into a student model using the remaining data [49].

Performance comparisons are depicted in Figure 5 for unlearning accuracy Δ_{acc} and detailed in Table 1 for unlearning speed. The results demonstrate that our method not only enhances unlearning

speed by up to 99% over alternative unlearning methods but also consistently outperforms them in unlearning accuracy.

These results indicate that our method exhibits outstanding effectiveness and efficiency in handling the complexity of model unlearning. In what follows, we evaluate the proposed parallel unlearning method in comparison with the most robust method—re-training. Within all considered learning frameworks, our proposed FIUn method achieves a maximum increase in unlearning speed of 99% compared to the re-training benchmark across different datasets and models. The detailed results are summarized in Tables 2 to 5, with more experiments provided in **Appendix .2.1**.

1) *Single-label unlearning*. For all frameworks and model types in CIFAR100, experimental results show that the AD_f metric reaches 0, strongly proving that our method effectively unlearns single-class labels. Meanwhile, the average AD_r metric is as high as 94.53%, further confirming our method’s efficiency in retaining labels. For all frameworks and model types in TinyImageNet, the AD_f metric also reaches 0, and the average AD_r metric reaches 79.49%. This significantly validates the effectiveness of our method.

2) *Multi-label unlearning*. For the CIFAR100 dataset, with $\#C_f = 2, 4, 10$, the average AD_f metric across all frameworks and model types is 1.93%, while the average AD_r metric reaches 86.01%. For the TinyImageNet dataset, the average AD_f metric is 0.21%, and the average AD_r metric is 83.54%. These results further demonstrate the effectiveness of our method. On the other hand, for both the IL and TL frameworks, as the number of unlearning label classes increases, the AD_f metric for all models approaches 0. However, the AD_r performance of the AlexNet and DenseNet161 models shows a downward trend, while the AD_r performance of the ResNet18 model remains stable.

Further observation reveals that the number of parameters in the last layer of DenseNet161 is 4.3 times that of ResNet18, and the number of parameters in the last layer of AlexNet is 7.9 times that of ResNet18. These results indicate that as the number of model parameters and the classes of forgotten labels increases, the AD_r performance may decline. This further suggests that while our proposed method effectively unlearns specified labels, it can somewhat affect the accuracy of retained labels.

6.2 Merged Label Unlearning Analysis

This section assesses the applicability of the merging FIM function to models with various distributions of unlearned labels. We analyze the unlearning performance of different types of models across various datasets within the FL and DDPL frameworks. As demonstrated in Tables 6 and 7, with more experiments provided in **Appendix .2.2**, the average AD_r is 89.72%, and the average AD_f is 5.62%, confirming the unlearning effectiveness of our method. We further validate that in the FIM, the impact of data on model parameters remains relatively stable.

We also analyze whether our proposed merging FIM function can handle the merged label unlearning task within the FL framework. As illustrated in Figure 7, in the AlexNet and DenseNet161 models, our method shows an average performance improvement of 88.54%, compared to using FIM directly. In the ResNet18 model, our method’s performance closely matches that of FIM. Additionally, our proposed merged label unlearning is, on average, 2.3 times

faster than general label unlearning. This further validates the efficiency of our method.

6.3 Inherited Depth of Model Analysis

We further examine whether the performance of FIUn is influenced by the increasing depth of inheritance within the FL and IL frameworks. All experiments are conducted with the same hyper-parameters.

- **Federated Learning**. In the FL framework, the CIFAR100 and TinyImageNet datasets are randomly divided into five segments. Each model trains using one segment of the data, adopting a binary tree structure as depicted in Figure 6(d). We evaluate whether our method can effectively unlearn specified labels as the depth of the binary tree increases.
- **Incremental Learning**. In the IL framework, as demonstrated in Figure 6(c), the starting model w_g contains data from 170 classes. With each incremental learning step, one class of label data is added to assess whether our method can effectively unlearn specified labels.

As shown in Figure 8 (i.e., single-class unlearning, see **Appendix .4**), we observe that under both frameworks, various datasets, and models with different unlearned labels, the performance of the proposed algorithm remains consistent regardless of the increased inherited depth. This consistency across both frameworks and models supports the notion that the impact of data on model parameters remains stable at fixed positions. Such stability ensures that our method maintains high performance even as the depth increases.

6.4 Analysis of Parameter Layer Selection in Models

We analyze how the number of model layers used to calculate the FIM impacts the performance of our algorithm. We conduct experiments within both FL and IL frameworks, with 15 label categories selected as unlearned labels. The DAG diagrams for these frameworks are illustrated in Figures 6(a) and 6(c). We calculate the FIM using the last layer, the last four layers, the last seven layers, and all layers to assess unlearning performance.

As depicted in Figure 9, we observe that an increase in the number of layers used leads to diminishing unlearning performance across various datasets and models. This decline is attributable to the increase in the layer parameters, which inversely affects the AD_r and AD_f metrics. Moreover, a larger number of layers prolongs the time needed to compute the FIM. This finding underscores the effectiveness of our method, which relies on calculations from only the last layer.

7 RELATED WORK

Although FL [34], DDPL [33], IL [55], and TL [58] have each made significant strides in addressing specific challenges, such as data privacy protection [32], model training efficiency [10], knowledge retention and unlearning [18], and cross-domain knowledge transfer [46], systematic exploration that combines these learning frameworks remains sparse. Most studies have merely attempted simple combinations of a few methods [8, 9, 41, 61] without touching the core of their commonality–model inheritance. This characteristic

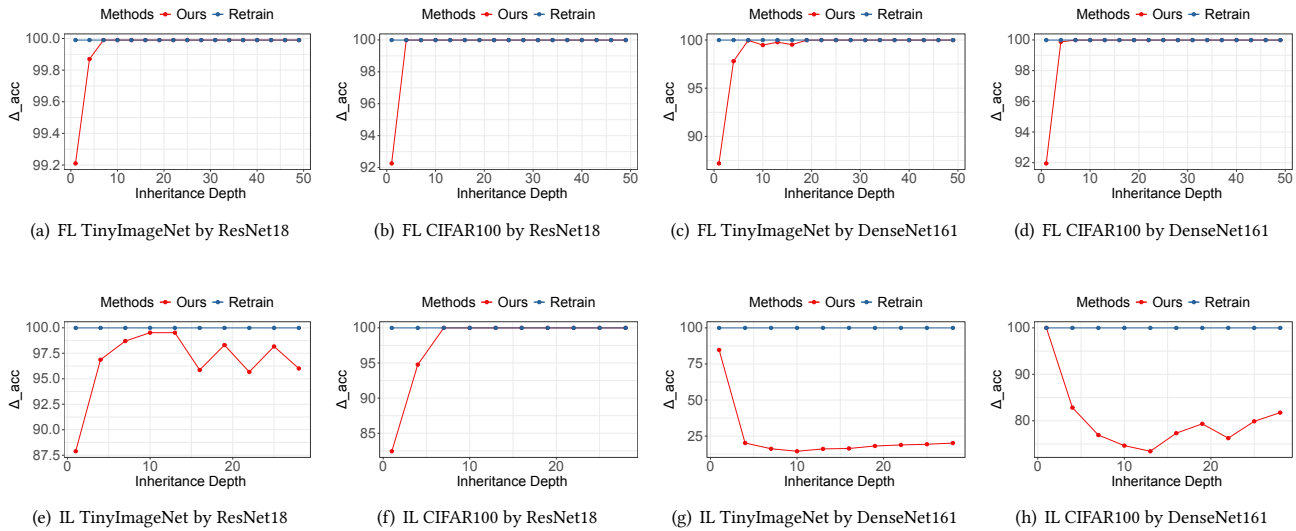


Figure 8: Inheritance depth analysis $\#C_f = 4$.

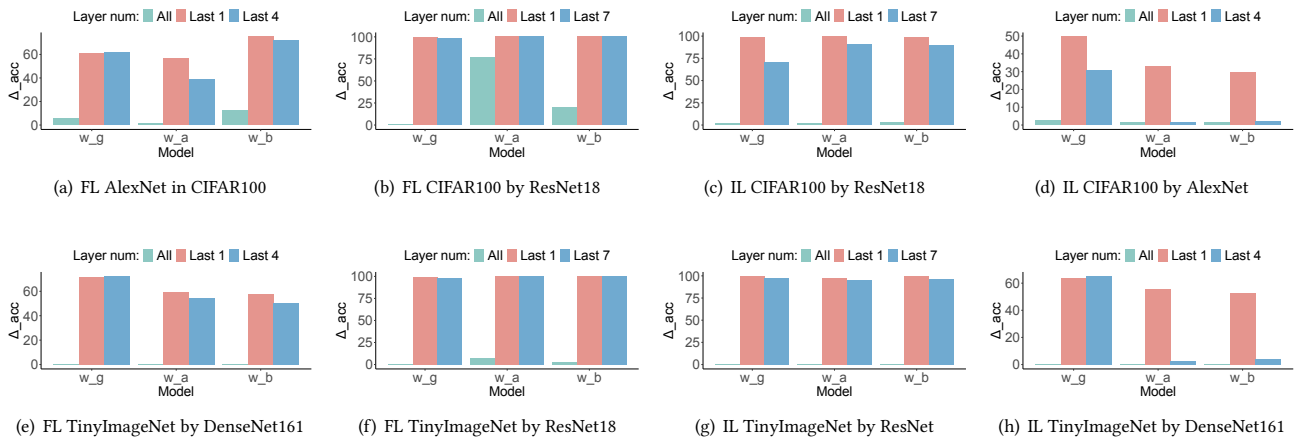


Figure 9: Unlearning layer analysis $\#C_f = 15$.

plays a crucial role in environments where unlearning is conducted on a large-scale. As data and models grow, the computational overhead increases exponentially with the depth of inheritance, while time consumption grows linearly with the depth, even when unlearning can be executed simultaneously at the same depth starting from the unlearning origin. This holds true regardless of the existing unlearning methods utilized, which are respectively discussed in the following.

Federated Unlearning. FedEraser [35] used historical parameter updates from the central server to reconstruct the deleted model. Wu et al. [60] subtracted historical updates and used knowledge distillation to restore model performance without client data. FRU [63] recalled and calibrated historical updates to eliminate user contributions and accelerate federated recommendation reconstruction. These methods primarily relied on recalling and calibrating historical parameter updates of the model to achieve deletion or

re-training. Halimi et al. [17] reversed the learning process by maximizing local empirical loss and used PGD to perform deletion on the client side, while Wu et al. [59] used class, client, and sample decoupling learning combined with Stochastic Gradient Ascent (SGA) and Elastic Weight Consolidation (EWC) to achieve deletion. These methods achieved deletion by optimizing the model's loss function or gradients.

Liu et al. [38] utilized first-order Taylor expansion and a diagonal empirical Fisher information matrix for accelerated re-training. Wang et al. [57] applied CNN channel pruning to remove specific category information, while FFMU [6] employed nonlinear function analysis to enhance model deletion processes. These approaches streamline deletion or re-training by altering the model structure or employing targeted techniques. Additionally, KNOT [51] optimized re-training by introducing clustering aggregation and framing the client clustering issue as a dictionary minimization problem.

Distributed Data-Parallel Unlearning. In DDPL knowledge unlearning, handling the unlearning process is restricted to the data shard on the specific device, followed by model aggregation and iterative training. If unlearning is required from a specific shard, only the model trained on that shard is re-trained. Approximate machine unlearning directly modifies trained model parameters, employing methods such as 1) Gradient-based approaches [11, 16, 42], which update model gradients to gradually diminish the data's influence, and 2) Data perturbation [15, 53], which introduces noise to reduce specific data points' impact on the model. These methods facilitate effective knowledge unlearning in DDPL.

Incremental Unlearning. Research on unlearning on IL is still nascent, yet the Projected-Gradient Unlearning method (PGU) [19] shows promise. PGU computes the gradients for the unlearning dataset and projects these onto the Core Gradient Space (CGS) derived from the training set. It then subtracts this projected component from the original gradients, positioning the residuals in a space orthogonal to the CGS, and updates the model parameters with these adjusted gradients. Effective for one-time data deletions and batch-wise unlearning, PGU is well-suited for ongoing incremental learning processes.

Transfer Unlearning. Research on unlearning specific target task knowledge has been relatively scarce in TL. To address this challenge, [48] proposed fine-tuning pre-trained models through data selection. Subsequently, the entire network was fine-tuned on the target task using gradient descent.

What Sets Our Solution Apart. The above-mentioned existing studies on unlearning methods typically endure high computational complexity, significant resource demands, and implementation difficulties. These methods are time-consuming and resource-intensive, especially when deployed in large-scale environments, as they require accurate tracking and sequential updating of numerous model parameters. By contrast, the proposed FIUn method fully parallelizes unlearning, significantly enhancing computational efficiency, resource utilization, and adaptability. It effectively addresses the challenges faced by existing unlearning methods in inheritance-oriented model networks.

8 CONCLUSION

In this paper, we developed a new parallel unlearning framework for models with dependence and inheritance. To do this, we introduced the UMIG, which can effectively abstract model inheritance, e.g., in FL, DDPL, IL, and TL, using a DAG topology. We also developed the FIUn method and the merging FIM function, which can quickly locate impacted models and conduct parallel unlearning through the UMIG. Experimental results on various models and datasets showed that our method achieves complete unlearning for single-class labels, while maintaining an average accuracy of 94.53% for retained labels. For multi-class labels, the unlearning accuracy is only 1.07%, with retained label accuracy at 84.77%. Our method is 99% faster than existing unlearning methods, efficiently handling model updates regardless of inheritance depth.

REFERENCES

[1] Martín Abadi, Paul Barham, Jianmin Chen, Zhifeng Chen, Andy Davis, Jeffrey Dean, Matthieu Devin, Sanjay Ghemawat, Geoffrey Irving, Michael Isard, et al.

2016. TensorFlow: a system for Large-Scale machine learning. In *12th USENIX symposium on operating systems design and implementation (OSDI 16)*, 265–283.
- [2] Abhishek Aich. 2021. Elastic weight consolidation (EWC): Nuts and bolts. *arXiv preprint arXiv:2105.04093* (2021).
- [3] Lucas Bourtole, Varun Chandrasekaran, Christopher A Choquette-Choo, Hengrui Jia, Adelin Travers, Baiwu Zhang, David Lie, and Nicolas Papernot. 2021. Machine unlearning. In *2021 IEEE Symposium on Security and Privacy (SP)*. IEEE, 141–159.
- [4] Mingrui Cao, Bin Cao, Wei Hong, Zhongyuan Zhao, Xiang Bai, and Lei Zhang. 2021. DAG-FL: Direct acyclic graph-based blockchain empowers on-device federated learning. In *ICC 2021-IEEE International Conference on Communications*. IEEE, 1–6.
- [5] Mingrui Cao, Long Zhang, and Bin Cao. 2021. Toward on-device federated learning: A direct acyclic graph-based blockchain approach. *IEEE Transactions on Neural Networks and Learning Systems* 34, 4 (2021), 2028–2042.
- [6] Tianshi Che, Yang Zhou, Zijie Zhang, Lingjuan Lyu, Ji Liu, Da Yan, Dejing Dou, and Jun Huan. 2023. Fast federated machine unlearning with nonlinear functional theory. In *International conference on machine learning*. PMLR, 4241–4268.
- [7] Yun-Wei Chu, Seyyedali Hosseinalipour, Elizabeth Tenorio, Laura Cruz, Kerrie Douglas, Andrew S Lan, and Christopher G Brinton. 2024. Multi-layer personalized federated learning for mitigating biases in student predictive analytics. *IEEE Transactions on Emerging Topics in Computing* (2024).
- [8] Jason Jinquan Dai, Yiheng Wang, Xin Qiu, Ding Ding, Yao Zhang, Yanzhang Wang, Xianyan Jia, Cherry Li Zhang, Yan Wan, Zhichao Li, et al. 2019. Bigdl: A distributed deep learning framework for big data. In *Proceedings of the ACM Symposium on Cloud Computing*, 50–60.
- [9] Shuang Dai and Fanlin Meng. 2023. Addressing modern and practical challenges in machine learning: A survey of online federated and transfer learning. *Applied Intelligence* 53, 9 (2023), 11045–11072.
- [10] Jeffrey Dean, Greg Corrado, Rajat Monga, Kai Chen, Matthieu Devin, Mark Mao, Marc'aurilio Ranzato, Andrew Senior, Paul Tucker, Ke Yang, et al. 2012. Large scale distributed deep networks. *Advances in neural information processing systems* 25 (2012).
- [11] Chongyu Fan, Jiancheng Liu, Yihua Zhang, Dennis Wei, Eric Wong, and Sijia Liu. 2023. Salun: Empowering machine unlearning via gradient-based weight saliency in both image classification and generation. *arXiv preprint arXiv:2310.12508* (2023).
- [12] Jack Foster, Kyle Fogarty, Stefan Schoepf, Cengiz Öztireli, and Alexandra Brintrup. 2024. Zero-shot machine unlearning at scale via lipschitz regularization. *arXiv preprint arXiv:2402.01401* (2024).
- [13] Jack Foster, Stefan Schoepf, and Alexandra Brintrup. 2024. Fast machine unlearning without retraining through selective synaptic dampening. In *Proceedings of the AAAI Conference on Artificial Intelligence*, Vol. 38. 12043–12051.
- [14] Keshi Ge, Kai Lu, Yongquan Fu, Xiaoge Deng, Zhiquan Lai, and Dongsheng Li. 2023. Compressed Collective Sparse-Sketch for Distributed Data-Parallel Training of Deep Learning Models. *IEEE Journal on Selected Areas in Communications* 41, 4 (2023), 941–963.
- [15] Shashwat Goel, Ameya Prabhu, Philip Torr, Ponnurangam Kumaraguru, and Amartya Sanyal. 2024. Corrective Machine Unlearning. *arXiv preprint arXiv:2402.14015* (2024).
- [16] Aditya Golatkar, Alessandro Achille, and Stefano Soatto. 2020. Eternal sunshine of the spotless net: Selective forgetting in deep networks. In *Proceedings of the IEEE/CVF Conference on Computer Vision and Pattern Recognition*. 9304–9312.
- [17] Anisa Halimi, Swanand Kadhe, Ambrish Rawat, and Nathalie Baracaldo. 2022. Federated unlearning: How to efficiently erase a client in fl? *arXiv preprint arXiv:2207.05521* (2022).
- [18] Dongqi Han, Zhiliang Wang, Wenqi Chen, Kai Wang, Rui Yu, Su Wang, Han Zhang, Zhihua Wang, Minghui Jin, Jiahai Yang, et al. 2023. Anomaly Detection in the Open World: Normality Shift Detection, Explanation, and Adaptation.. In *NDSS*.
- [19] Tuan Hoang, Santu Rana, Sunil Gupta, and Svetha Venkatesh. 2024. Learn to unlearn for deep neural networks: Minimizing unlearning interference with gradient projection. In *Proceedings of the IEEE/CVF Winter Conference on Applications of Computer Vision*. 4819–4828.
- [20] Forrest N Iandola, Song Han, Matthew W Moskewicz, Khalid Ashraf, William J Dally, and Kurt Keutzer. 2016. SqueezeNet: AlexNet-level accuracy with 50x fewer parameters and < 0.5 MB model size. *arXiv preprint arXiv:1602.07360* (2016).
- [21] Bargav Jayaraman and David Evans. 2019. Evaluating differentially private machine learning in practice. In *28th USENIX Security Symposium (USENIX Security 19)*. 1895–1912.
- [22] Hyunjune Kim, Sangyong Lee, and Simon S Woo. 2024. Layer Attack Unlearning: Fast and Accurate Machine Unlearning via Layer Level Attack and Knowledge Distillation. In *Proceedings of the AAAI Conference on Artificial Intelligence*, Vol. 38. 21241–21248.
- [23] Junyaup Kim and Simon S Woo. 2022. Efficient two-stage model retraining for machine unlearning. In *Proceedings of the IEEE/CVF Conference on Computer Vision and Pattern Recognition*. 4361–4369.

- [24] James Kirkpatrick, Razvan Pascanu, Neil Rabinowitz, Joel Veness, Guillaume Desjardins, Andrei A Rusu, Kieran Milan, John Quan, Tiago Ramalho, Agnieszka Grabska-Barwinska, et al. 2017. Overcoming catastrophic forgetting in neural networks. *Proceedings of the national academy of sciences* 114, 13 (2017), 3521–3526.
- [25] Torsten Krauß, Jan König, Alexandra Dmitrienko, and Christian Kanzow. 2024. Automatic Adversarial Adaption for Stealthy Poisoning Attacks in Federated Learning. NDSS.
- [26] Dominik Kreuzberger, Niklas Kühl, and Sebastian Hirschl. 2023. Machine Learning Operations (MLOps): Overview, Definition, and Architecture. *IEEE Access* 11 (2023), 31866–31879. <https://doi.org/10.1109/ACCESS.2023.3262138>
- [27] Alex Krizhevsky, Geoffrey Hinton, et al. 2009. Learning multiple layers of features from tiny images. (2009).
- [28] Ya Le and Xuan Yang. 2015. Tiny imagenet visual recognition challenge. *CS 231N* 7, 7 (2015), 3.
- [29] Sunwoo Lee, Tuo Zhang, and A Salman Avestimehr. 2023. Layer-wise adaptive model aggregation for scalable federated learning. In *Proceedings of the AAAI Conference on Artificial Intelligence*. Vol. 37. 8491–8499.
- [30] Li Li, Yuxi Fan, Mike Tse, and Kuo-Yi Lin. 2020. A review of applications in federated learning. *Computers & Industrial Engineering* 149 (2020), 106854.
- [31] Mu Li, Tong Zhang, Yuqiang Chen, and Alexander J Smola. 2014. Efficient mini-batch training for stochastic optimization. In *Proceedings of the 20th ACM SIGKDD international conference on Knowledge discovery and data mining*. 661–670.
- [32] Qinbin Li, Zeyi Wen, Zhaomin Wu, Sixu Hu, Naibo Wang, Yuan Li, Xu Liu, and Bingsheng He. 2021. A survey on federated learning systems: Vision, hype and reality for data privacy and protection. *IEEE Transactions on Knowledge and Data Engineering* 35, 4 (2021), 3347–3366.
- [33] Shen Li, Yanli Zhao, Rohan Varma, Omkar Salpekar, Pieter Noordhuis, Teng Li, Adam Paszke, Jeff Smith, Brian Vaughan, Pritam Damania, et al. 2020. Pytorch distributed: Experiences on accelerating data parallel training. *arXiv preprint arXiv:2006.15704* (2020).
- [34] Tian Li, Anit Kumar Sahu, Manzil Zaheer, Maziar Sanjabi, Ameet Talwalkar, and Virginia Smith. 2020. Federated optimization in heterogeneous networks. *Proceedings of Machine learning and systems 2* (2020), 429–450.
- [35] Gaoyang Liu, Xiaoqiang Ma, Yang Yang, Chen Wang, and Jiangchuan Liu. 2020. Federated unlearning. *arXiv preprint arXiv:2012.13891* (2020).
- [36] Jiancheng Liu, Parikshit Ram, Yuguang Yao, Gaowen Liu, Yang Liu, PRANAY SHARMA, Sijia Liu, et al. 2024. Model sparsity can simplify machine unlearning. *Advances in Neural Information Processing Systems* 36 (2024).
- [37] Xiao Liu, Mingyuan Li, Xu Wang, Guangsheng Yu, Wei Ni, Lixiang Li, Haipeng Peng, and Renping Liu. 2024. Decentralized Federated Unlearning on Blockchain. *arXiv preprint arXiv:2402.16294* (2024).
- [38] Yi Liu, Lei Xu, Xingliang Yuan, Cong Wang, and Bo Li. 2022. The right to be forgotten in federated learning: An efficient realization with rapid retraining. In *IEEE INFOCOM 2022-IEEE Conference on Computer Communications*. IEEE, 1749–1758.
- [39] Beatriz M. A. Matsui and Denise H. Goya. 2023. MLOps: a guide to its adoption in the context of responsible AI. In *Proceedings of the 1st Workshop on Software Engineering for Responsible AI (Pittsburgh, Pennsylvania) (SE4RAI '22)*. Association for Computing Machinery, New York, NY, USA, 45–49. <https://doi.org/10.1145/3526073.3527591>
- [40] Brendan McMahan, Eider Moore, Daniel Ramage, Seth Hampson, and Blaise Aguerre y Arcas. 2017. Communication-efficient learning of deep networks from decentralized data. In *Artificial intelligence and statistics*. PMLR, 1273–1282.
- [41] Qinghai Miao, Yisheng Lv, Min Huang, Xiao Wang, and Fei-Yue Wang. 2023. Parallel learning: Overview and perspective for computational learning across Syn2Real and Sim2Real. *IEEE/CAA Journal of Automatica Sinica* 10, 3 (2023), 603–631.
- [42] Seth Neel, Aaron Roth, and Saeed Sharifi-Malvajerdi. 2021. Descent-to-delete: Gradient-based methods for machine unlearning. In *Algorithmic Learning Theory*. PMLR, 931–962.
- [43] Modupe Odusami, Rytis Maskeliūnas, Robertas Damaševičius, and Tomas Krilavičius. 2021. Analysis of features of Alzheimer’s disease: Detection of early stage from functional brain changes in magnetic resonance images using a finetuned ResNet18 network. *Diagnostics* 11, 6 (2021), 1071.
- [44] Adam Paszke, Sam Gross, Francisco Massa, Adam Lerer, James Bradbury, Gregory Chanan, Trevor Killeen, Zeming Lin, Natalia Gimelshein, Luca Antiga, et al. 2019. Pytorch: An imperative style, high-performance deep learning library. *Advances in neural information processing systems* 32 (2019).
- [45] Antonio Polino, Razvan Pascanu, and Dan Alistarh. 2018. Model compression via distillation and quantization. In *International Conference on Learning Representations*.
- [46] Sampath Rajapaksha, Harsha Kalutarage, M Omar Al-Kadri, Andrei Petrovski, and Garikayi Madzudzo. 2023. Improving in-vehicle networks intrusion detection using on-device transfer learning. In *Symposium on vehicles security and privacy*, Vol. 10.
- [47] Christoph Sendner, Huili Chen, Hossein Fereidooni, Lukas Petzi, Jan König, Jasper Stang, Alexandra Dmitrienko, Ahmad-Reza Sadeghi, and Farinaz Koushanfar. 2023. Smarter Contracts: Detecting Vulnerabilities in Smart Contracts with Deep Transfer Learning. In NDSS.
- [48] Nazanin Mohammadi Sepahvand, Vincent Dumoulin, Eleni Triantafyllou, and Gintare Karolina Dziugaite. 2024. Data Selection for Transfer Unlearning. *arXiv preprint arXiv:2405.10425* (2024).
- [49] Yash Sinha, Murari Mandal, and Mohan Kankanhalli. 2023. Distill to Delete: Unlearning in Graph Networks with Knowledge Distillation. *arXiv preprint arXiv:2309.16173* (2023).
- [50] M Kay Steven. 1993. Fundamentals of statistical signal processing. *PTR Prentice-Hall, Englewood Cliffs, NJ* 10, 151045 (1993), 148.
- [51] Ningxin Su and Baochun Li. 2023. Asynchronous federated unlearning. In *IEEE INFOCOM 2023-IEEE Conference on Computer Communications*. IEEE, 1–10.
- [52] Muhammed Talo. 2019. Automated classification of histopathology images using transfer learning. *Artificial intelligence in medicine* 101 (2019), 101743.
- [53] Ayush K Tarun, Vikram S Chundawat, Murari Mandal, and Mohan Kankanhalli. 2023. Fast yet effective machine unlearning. *IEEE Transactions on Neural Networks and Learning Systems* (2023).
- [54] Muhammad Umer and Robi Polikar. 2021. Adversarial targeted forgetting in regularization and generative based continual learning models. In *2021 International Joint Conference on Neural Networks (IJCNN)*. IEEE, 1–8.
- [55] Gido M Van de Ven, Tinne Tuytelaars, and Andreas S Tolias. 2022. Three types of incremental learning. *Nature Machine Intelligence* 4, 12 (2022), 1185–1197.
- [56] Paul Voigt and Axel Von dem Bussche. 2017. The eu general data protection regulation (gdpr). *A Practical Guide, 1st Ed., Cham: Springer International Publishing* 10, 3152676 (2017), 10–5555.
- [57] Junxiao Wang, Song Guo, Xin Xie, and Heng Qi. 2022. Federated unlearning via class-discriminative pruning. In *Proceedings of the ACM Web Conference 2022*. 622–632.
- [58] Karl Weiss, Taghi M Khoshgoftaar, and DingDing Wang. 2016. A survey of transfer learning. *Journal of Big data* 3 (2016), 1–40.
- [59] Chen Wu, Sencun Zhu, and Prasenjit Mitra. 2022. Federated unlearning with knowledge distillation. *arXiv preprint arXiv:2201.09441* (2022).
- [60] Leijie Wu, Song Guo, Junxiao Wang, Zicong Hong, Jie Zhang, and Yaohong Ding. 2022. Federated unlearning: Guarantee the right of clients to forget. *IEEE Network* 36, 5 (2022), 129–135.
- [61] Jaehong Yoon, Wonyong Jeong, Giwoong Lee, Eunho Yang, and Sung Ju Hwang. 2021. Federated continual learning with weighted inter-client transfer. In *International Conference on Machine Learning*. PMLR, 12073–12086.
- [62] Guangsheng Yu, Xu Wang, Caijun Sun, Qin Wang, Ping Yu, Wei Ni, and Ren Ping Liu. 2023. Ironforge: An open, secure, fair, decentralized federated learning. *IEEE Transactions on Neural Networks and Learning Systems* (2023).
- [63] Wei Yuan, Hongzhi Yin, Fangzhao Wu, Shijie Zhang, Tiekhe He, and Hao Wang. 2023. Federated unlearning for on-device recommendation. In *Proceedings of the Sixteenth ACM International Conference on Web Search and Data Mining*. 393–401.
- [64] Ke Zhang, Carl Yang, Xiaoxiao Li, Lichao Sun, and Siu Ming Yiu. 2021. Sub-graph federated learning with missing neighbor generation. *Advances in Neural Information Processing Systems* 34 (2021), 6671–6682.
- [65] Ruiqi Zhang, Licong Lin, Yu Bai, and Song Mei. 2024. Negative preference optimization: From catastrophic collapse to effective unlearning. *arXiv preprint arXiv:2404.05868* (2024).

1 Experiment Hyperparameters

Table 8 summarizes the hyperparameters for FIUn, AlexNet, DenseNet161, and ResNet18 used in our experiments.

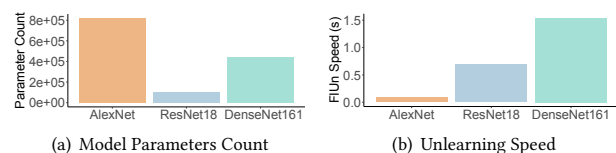


Figure 10: Parameters of the last layer and FIUn unlearning speed of different types of models. FIUn speed is based on the FL framework with CIFAR100.

Table 8: Hyperparameters

Hyperparameter Types	Hyperparameter	Settings
FIUn hyperparameter	optimizer	SGD
	learning rate	0.1
	epochs	100
	batch size	64
	τ	1
	γ	1
	η	0.1
	use layer	last layer
AlexNet hyperparameter	optimizer	SGD
	learning rate	0.01
	epochs	200
	batch size	64
DenseNet161 hyperparameter	optimizer	SGD
	learning rate	0.01
	epochs	100
	batch size	64
ResNet18 hyperparameter	optimizer	SGD
	learning rate	0.1
	epochs	100
	batch size	64

.2 More Experiments of learning frameworks

.2.1 General Label Unlearning Analysis. Table 9 to Table 12 show that, on CIFAR-100, federated unlearning and incremental unlearning demonstrate good performance. Similarly, on TinyImageNet, transfer unlearning and distributed data-parallel unlearning exhibit excellent performance. Re-training on TinyImageNet takes

a significantly longer time than CIFAR-100. In comparison, our proposed FIUn maintains high unlearning accuracy while keeping the unlearning time extremely short.

.2.2 Merged Label Unlearning Analysis. Tables 13 and 14 show that, on CIFAR100, federated unlearning shows good performance on multi-label distributions. On TinyImageNet, distributed data-parallel unlearning demonstrates excellent performance on multi-label distributions. For multiple label distributions, our proposed MFIM function accelerates the unlearning speed of inherited models while maintaining high unlearning accuracy.

.3 Unlearning Speed Analysis

Figure 10 shows that the parameters of the last layer are not directly related to the training speed. Moreover, ResNet18 trains much more slowly than AlexNet because ResNet18 has a deeper architecture, while AlexNet has fewer layers and larger convolutional kernels, leading to a lower computational load. DenseNet161 is slower than ResNet18 because DenseNet161 employs a feature reuse mechanism requiring frequent memory access, resulting in comparatively slower training speed.

.4 Inherited Depth of Model Analysis

Figure 11 focuses on the performance of inheritance depth under single-class unlearning, revealing that even under these conditions, it still exhibits excellent unlearning capability similar to multi-class unlearning. This unlearning capability does not diminish with the increasing inherent depth of the model; in this sense, the impact of data on model parameters remains stable at fixed positions.

Table 9: Federated Unlearning Performance On CIFAR-100

Model	# C_f	Metrics	Original Model (%)			Re-training Model (%)			FIUn (%)			Cumulative Unlearning Time (s)					
												Re-training			FIUn		
			w_g	w_a	w_b	w_g	w_a	w_b	w_g	w_a	w_b	w_g	w_a	w_b	w_g	w_a	w_b
AlexNet	1	$AD_r \uparrow$	99.99	99.99	99.81	99.99	99.99	98.80	97.13	96.41	97.12	29.70	59.06	89.62	0.09	0.11	0.13
		$AD_f \downarrow$	99.99	99.99	99.66	0.00	0.00	0.00	0.00	0.00	0.00						
	2	$AD_r \uparrow$	99.99	99.99	99.86	99.99	99.99	99.51	91.89	90.78	95.66	28.69	57.81	84.97	0.11	0.16	0.13
		$AD_f \downarrow$	99.99	99.99	99.49	0.00	0.00	0.00	0.00	0.00	0.00						
	4	$AD_r \uparrow$	99.99	99.99	99.96	99.99	99.99	99.16	85.79	78.54	89.40	26.39	53.10	81.96	0.10	0.16	0.13
		$AD_f \downarrow$	99.99	99.99	99.89	0.00	0.00	0.00	0.00	0.00	0.00						
	10	$AD_r \uparrow$	99.99	99.99	99.72	99.71	92.72	90.84	82.26	71.31	89.39	21.96	42.37	63.82	0.11	0.14	0.15
		$AD_f \downarrow$	99.99	99.99	98.82	0.00	0.00	0.00	9.29	9.29	10.68						
ResNet18	1	$AD_r \uparrow$	99.99	99.99	99.99	99.99	99.99	99.99	97.09	97.13	96.93	30.36	61.40	90.94	0.68	1.00	0.99
		$AD_f \downarrow$	99.99	99.99	99.99	0.00	0.00	0.00	0.00	0.00	0.00						
	2	$AD_r \uparrow$	99.99	99.99	99.99	99.99	99.99	99.99	96.66	98.10	97.44	28.30	57.39	84.06	0.69	1.03	1.09
		$AD_f \downarrow$	99.99	99.99	99.99	0.00	0.00	0.00	0.00	0.00	0.00						
	4	$AD_r \uparrow$	99.99	99.99	99.99	99.96	99.99	99.99	97.17	99.45	99.19	26.39	52.69	81.39	0.75	1.09	1.06
		$AD_f \downarrow$	99.99	99.99	99.99	0.00	0.00	0.00	0.00	0.00	0.00						
	10	$AD_r \uparrow$	99.99	99.99	99.99	99.99	99.99	99.99	99.02	99.99	99.99	22.03	44.83	66.30	0.76	1.14	1.04
		$AD_f \downarrow$	99.99	99.99	99.99	0.00	0.00	0.00	0.00	0.00	0.00						

Table 10: Incremental Unlearning Performance On CIFAR-100

Model	# C_f	Metrics	Original Model (%)			Re-training Model (%)			FIUn (%)			Cumulative Unlearning Time (s)					
												Re-training			FIUn		
			w_g	w_a	w_b	w_g	w_a	w_b	w_g	w_a	w_b	w_g	w_a	w_b	w_g	w_a	w_b
AlexNet	1	$AD_r \uparrow$	99.99	99.99	99.81	99.99	99.99	98.80	98.97	94.39	94.98	22.95	43.83	63.45	0.09	0.39	0.39
		$AD_f \downarrow$	99.99	99.99	99.66	0.00	0.00	0.00	0.00	0.00	0.00						
	2	$AD_r \uparrow$	99.99	99.99	99.80	99.99	99.99	99.51	92.93	71.58	69.14	21.35	41.58	62.10	0.11	0.27	0.26
		$AD_f \downarrow$	99.99	99.99	99.49	0.00	0.00	0.00	0.00	0.00	0.00						
	4	$AD_r \uparrow$	99.99	99.99	99.96	99.99	99.99	99.16	88.77	59.62	58.81	20.52	41.12	60.69	0.12	0.28	0.29
		$AD_f \downarrow$	99.99	99.99	99.89	0.00	0.00	0.00	0.00	0.00	0.00						
	10	$AD_r \uparrow$	99.99	99.99	99.72	99.99	99.99	99.99	87.55	45.12	40.91	17.35	38.32	57.94	0.12	0.28	0.29
		$AD_f \downarrow$	99.99	99.99	98.82	0.00	0.00	0.00	18.88	0.00	0.00						
ResNet18	1	$AD_r \uparrow$	99.99	99.99	99.99	99.99	99.99	99.99	91.71	90.05	90.82	26.35	47.12	66.93	0.30	0.80	0.85
		$AD_f \downarrow$	99.99	99.99	99.99	0.00	0.00	0.00	0.00	0.00	0.00						
	2	$AD_r \uparrow$	99.99	99.99	99.99	99.99	99.99	99.99	91.49	89.02	87.64	25.37	45.93	65.89	0.30	0.84	0.85
		$AD_f \downarrow$	99.99	99.99	99.99	0.00	0.00	0.00	0.00	0.00	0.00						
	4	$AD_r \uparrow$	99.99	99.99	99.99	99.96	99.99	99.99	84.71	83.42	84.54	24.83	43.23	65.38	0.31	0.86	0.87
		$AD_f \downarrow$	99.99	99.99	99.99	0.00	0.00	0.00	0.00	0.00	0.00						
	10	$AD_r \uparrow$	99.99	99.99	99.99	99.99	99.99	99.99	82.42	80.56	81.30	18.93	39.93	58.93	0.32	0.88	0.89
		$AD_f \downarrow$	99.99	99.99	99.99	0.00	0.00	0.00	0.00	0.00	0.00						

Table 11: Transfer Unlearning Performance On TinyImageNet

Model	# C_f	Metrics	Original Model (%)			Re-training Model (%)			FIUn (%)			Cumulative Unlearning Time (s)					
			w_g	w_a	w_b	w_g	w_a	w_b	w_g	w_a	w_b	Re-training			FIUn		
												w_g	w_a	w_b	w_g	w_a	w_b
DenseNet161	1	$AD_r \uparrow$	86.33	91.24	89.34	97.75	97.52	96.75	71.49	69.82	66.73	987.94	1986.35	1985.16	2.41	4.15	4.34
		$AD_f \downarrow$	94.50	94.50	96.70	0.00	0.00	0.00	0.00	0.00	0.00						
	4	$AD_r \uparrow$	86.33	91.24	89.34	96.42	96.41	95.13	64.24	55.32	51.18	1001.34	1994.53	1986.61	2.34	4.71	4.26
		$AD_f \downarrow$	89.12	91.23	91.84	0.00	0.00	0.00	0.00	0.00	0.00						
	6	$AD_r \uparrow$	86.33	91.24	89.34	95.72	95.43	93.58	58.69	47.38	42.57	1018.14	2008.89	2009.31	2.16	4.64	4.46
		$AD_f \downarrow$	86.57	89.25	90.28	0.00	0.00	0.00	0.00	0.00	0.00						
	10	$AD_r \uparrow$	86.33	91.24	89.34	93.64	93.46	92.03	56.21	41.37	36.91	1034.30	2057.32	2051.86	2.64	4.84	4.16
		$AD_f \downarrow$	83.81	89.12	89.88	0.00	0.00	0.00	0.00	0.00	0.00						
ResNet18	1	$AD_r \uparrow$	99.99	99.99	99.99	99.99	99.99	99.99	98.66	98.07	96.74	142.15	243.75	241.61	0.42	0.75	0.78
		$AD_f \downarrow$	99.99	99.99	99.99	0.00	0.00	0.00	0.00	0.00	0.00						
	4	$AD_r \uparrow$	99.99	99.99	99.99	99.99	99.99	99.99	98.84	98.38	97.38	143.46	244.34	245.74	0.42	0.74	0.75
		$AD_f \downarrow$	99.99	99.99	99.99	0.00	0.00	0.00	0.00	0.00	0.00						
	6	$AD_r \uparrow$	99.96	99.99	99.99	99.99	99.99	99.99	98.82	98.91	98.98	147.27	245.35	246.41	0.56	0.89	0.74
		$AD_f \downarrow$	99.99	99.99	99.99	0.00	0.00	0.00	0.00	0.00	0.00						
	10	$AD_r \uparrow$	99.96	99.99	99.99	99.78	99.73	99.31	99.33	99.57	99.42	148.64	252.34	253.30	0.49	0.78	0.74
		$AD_f \downarrow$	99.99	99.99	99.99	0.00	0.00	0.00	0.00	0.00	0.00						

Table 12: Distributed Data-Parallel Unlearning Performance On TinyImageNet

Model	# C_f	Metrics	Original Model (%)			Re-training Model (%)			FIUn (%)			Cumulative Unlearning Time (s)					
			w_g	w_a	w_b	w_g	w_a	w_b	w_g	w_a	w_b	Re-training			FIUn		
												w_g	w_a	w_b	w_g	w_a	w_b
DenseNet161	1	$AD_r \uparrow$	99.99	87.16	85.21	99.99	89.39	87.24	91.82	86.63	83.58	980.53	988.42	991.75	2.13	2.61	4.34
		$AD_f \downarrow$	99.99	92.75	90.41	0.00	0.00	0.00	0.00	0.00	0.00						
	4	$AD_r \uparrow$	99.96	87.00	85.21	99.96	88.35	89.34	87.42	86.56	84.37	1004.63	1006.32	1005.332	2.35	2.05	4.31
		$AD_f \downarrow$	99.96	86.97	88.85	0.00	0.00	0.00	0.00	0.00	0.00						
	6	$AD_r \uparrow$	99.99	87.00	85.21	99.96	87.96	88.15	82.50	86.82	84.47	1024.25	1036.14	1026.74	2.21	2.24	4.16
		$AD_f \downarrow$	99.99	89.35	86.08	0.00	0.00	0.00	0.00	0.00	0.00						
	10	$AD_r \uparrow$	99.99	87.00	85.21	99.99	89.27	87.37	81.11	86.93	85.52	1048.32	1045.63	1046.65	2.35	2.26	4.31
		$AD_f \downarrow$	99.99	86.94	82.46	0.00	0.00	0.00	0.00	2.86	0.76						
ResNet18	1	$AD_r \uparrow$	99.99	99.99	99.99	99.99	99.99	99.99	99.19	99.99	99.99	112.52	117.34	114.52	1.47	1.67	3.56
		$AD_f \downarrow$	99.99	99.99	99.99	0.00	0.00	0.00	0.00	0.00	0.00						
	4	$AD_r \uparrow$	99.99	99.99	99.99	99.99	99.99	99.99	99.99	99.99	99.99	109.32	108.74	110.53	1.37	1.74	3.54
		$AD_f \downarrow$	99.99	99.99	99.99	0.00	0.00	0.00	0.00	0.00	0.32						
	6	$AD_r \uparrow$	99.96	99.99	99.99	99.96	99.96	99.96	99.38	99.99	99.99	107.78	108.32	107.17	1.64	1.84	3.53
		$AD_f \downarrow$	99.99	99.99	99.99	0.00	0.00	0.00	0.00	0.00	0.00						
	10	$AD_r \uparrow$	99.96	99.99	99.99	99.96	99.96	99.96	98.99	99.99	99.99	106.13	105.18	108.31	1.74	1.46	3.52
		$AD_f \downarrow$	99.99	99.99	99.99	0.00	0.00	0.00	0.00	11.56	0.38						

Table 13: Federated Unlearning Performance On CIFAR-100 With Multiple Label Distribution

Model	# \cap_f	Metrics	Original Model (%)			Re-training Model (%)			FIUn (%)			Cumulative Unlearning Time (s)					
			w_g	w_a	w_b	w_g	w_a	w_b	w_g	w_a	w_b	Re-training			FIUn		
												w_g	w_a	w_b	w_g	w_a	w_b
AlexNet	60%	$AD_r \uparrow$	99.99	99.99	99.81	98.80	99.99	99.99	69.42	81.68	75.05	59.26	30.13	29.70	0.15	0.08	0.09
		$AD_f \downarrow$	99.99	99.99	99.66	0.00	0.00	0.00	0.00	0.00	0.00						
	40%	$AD_r \uparrow$	99.99	99.99	99.80	99.51	99.99	99.99	61.66	79.77	72.96	53.84	29.58	28.69	0.11	0.09	0.19
		$AD_f \downarrow$	99.99	99.99	99.49	0.00	0.00	0.00	0.00	0.00	0.00						
	20%	$AD_r \uparrow$	99.99	99.99	99.96	99.16	99.99	99.99	59.57	77.47	77.97	57.36	27.48	26.39	0.10	0.07	0.18
		$AD_f \downarrow$	99.99	99.99	99.89	0.00	0.00	0.00	0.12	0.00	0.00						
	0%	$AD_r \uparrow$	99.99	99.99	99.99	90.84	92.72	99.71	81.79	69.20	81.30	45.31	22.37	21.96	0.11	0.10	0.18
		$AD_f \downarrow$	99.99	99.99	98.82	0.00	0.00	0.00	0.12	0.00	0.00						
ResNet18	60%	$AD_r \uparrow$	99.99	99.99	99.99	99.99	99.99	99.99	93.15	98.76	97.81	67.31	33.18	30.36	0.60	0.32	0.29
		$AD_f \downarrow$	99.99	99.99	99.99	0.00	0.00	0.00	0.00	0.00	0.00						
	40%	$AD_r \uparrow$	99.99	99.99	99.99	99.99	99.99	99.99	93.78	99.04	98.98	52.33	28.13	28.30	0.59	0.34	0.30
		$AD_f \downarrow$	99.99	99.99	99.99	0.00	0.00	0.00	0.00	0.00	0.00						
	20%	$AD_r \uparrow$	99.99	99.99	99.99	99.96	99.99	99.99	88.54	98.79	98.62	56.61	23.37	26.39	0.58	0.28	0.30
		$AD_f \downarrow$	99.99	99.99	99.99	0.00	0.00	0.00	0.00	0.00	0.00						
	0%	$AD_r \uparrow$	99.99	99.99	99.99	99.99	99.99	99.99	94.58	98.97	96.94	46.42	24.36	22.03	0.64	0.37	0.32
		$AD_f \downarrow$	99.99	99.99	99.99	0.00	0.00	0.00	0.00	0.00	0.00						

Table 14: Distributed Data-Parallel Unlearning Performance On TinyImageNet With Multiple Label Distribution

Model	# \cap_f	Metrics	Original Model (%)			Re-training Model (%)			FIUn (%)			Unlearning Time (s)					
			r_g	r_a	r_b	r_g	r_a	r_b	r_g	r_a	r_b	Re-training			FIUn		
												r_g	r_a	r_b	r_g	r_a	r_b
DenseNet161	60%	$AD_r \uparrow$	99.99	99.99	99.99	99.99	99.99	99.99	76.86	89.47	82.53	994.32	998.46	1000.66	4.69	2.39	2.30
		$AD_f \downarrow$	99.99	99.99	99.99	0.00	0.00	0.00	0.00	0.00	0.00						
	40%	$AD_r \uparrow$	99.99	99.99	99.50	99.99	99.99	99.99	74.03	89.47	83.18	1010.45	1011.14	1009.53	4.12	2.69	2.14
		$AD_f \downarrow$	99.99	99.99	99.99	0.00	0.00	0.00	0.00	0.00	0.00						
	20%	$AD_r \uparrow$	99.99	99.99	99.99	99.99	99.99	99.99	73.48	89.13	83.78	1021.34	1020.67	1022.64	4.98	2.64	2.59
		$AD_f \downarrow$	99.99	99.99	99.91	0.00	0.00	0.00	0.00	0.00	0.00						
	0%	$AD_r \uparrow$	99.99	86.30	99.99	99.99	99.99	99.71	71.43	89.53	85.00	1046.14	1041.32	1039.64	4.40	2.42	2.21
		$AD_f \downarrow$	99.99	99.99	99.99	0.00	0.00	0.00	0.00	0.00	0.00						
ResNet18	60%	$AD_r \uparrow$	99.99	99.99	99.99	99.99	99.99	99.99	95.16	95.92	98.86	123.74	126.43	149.32	3.16	1.65	1.68
		$AD_f \downarrow$	99.99	99.99	99.99	0.00	0.00	0.00	0.00	0.00	0.00						
	40%	$AD_r \uparrow$	99.99	99.99	99.99	99.99	99.99	99.99	94.43	95.92	98.27	128.43	127.64	155.32	3.97	1.46	1.59
		$AD_f \downarrow$	99.99	99.99	99.99	0.00	0.00	0.00	0.00	0.00	0.00						
	20%	$AD_r \uparrow$	99.99	99.99	99.99	99.96	99.99	99.99	94.71	95.92	98.48	129.35	126.43	154.83	3.89	1.54	1.38
		$AD_f \downarrow$	99.99	99.99	99.99	0.00	0.00	0.00	0.00	0.00	0.00						
	0%	$AD_r \uparrow$	99.99	99.99	99.99	99.99	99.99	99.99	92.86	95.92	99.01	125.32	124.34	151.38	3.10	1.69	1.39
		$AD_f \downarrow$	99.99	99.99	99.99	0.00	0.00	0.00	0.00	0.00	0.00						

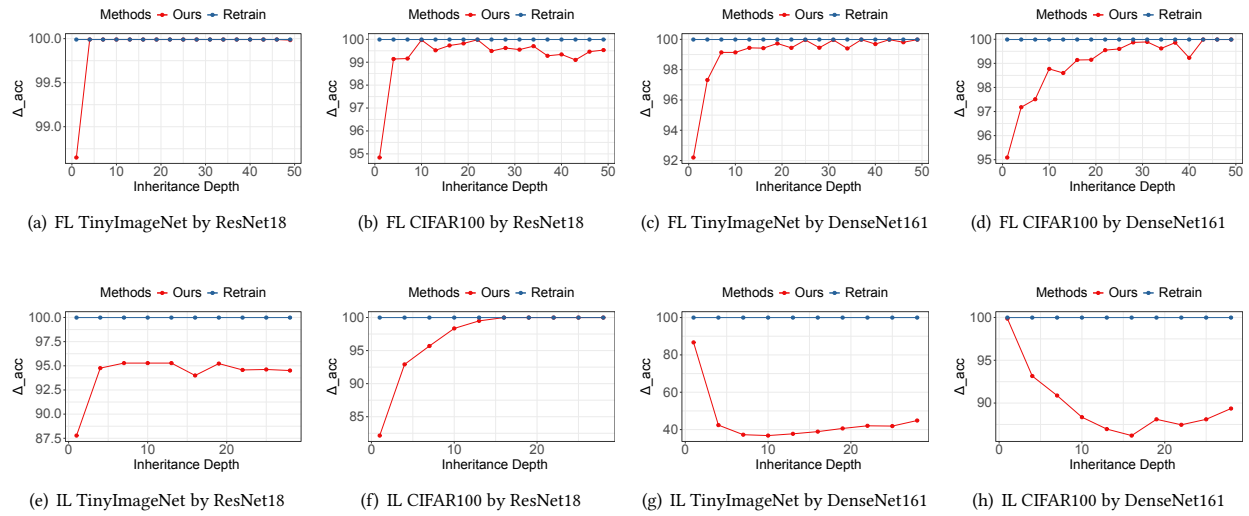


Figure 11: Inheritance depth analysis $\#C_f = 1$.